Успехи физ. мет. / Usp. Fiz. Met. 2010, т. 11, сс. 413–460
Оттиски доступны непосредственно от издателя
Фотокопирование разрешено только
в соответствии с лицензией

PACS numbers: 61.50.Ah, 61.50.Lt, 61.72.Bb, 64.60.Cn, 75.30.Et, 75.50.Bb, 81.30.Hd

Interatomic Interactions in F.C.C.-Ni–Fe Alloys

S. M. Bokoch[1,3,4,5] and V. A. Tatarenko[2,4]

[1]*Laboratoire Jean Kuntzmann, UMR 5224 CNRS,*
Tour IRMA, 51 rue des Mathematiques, B.P. 53,
F-38041 Grenoble Cedex 9, France
[2]*G. V. Kurdyumov Institute for Metal Physics, N.A.S.U.,*
Department of Solid State Theory,
Academician Vernadsky Blvd., 36,
UA-03680 Kyyiv-142, Ukraine
[3]*Paul-Drude-Institut für Festkörperelektronik,*
Hausvogteiplatz 5–7,
D-10117 Berlin, Germany
[4]*Taras Shevchenko Kyyiv National University,*
Physics Department,
Academician Glushkov Ave., 4,
UA-03022 Kyyiv, Ukraine
[5]*Groupe de Physique des Matériaux, UMR 6634 CNRS,*
Université de Rouen,
Ave. de l'Université, B.P. 12,
F-76801 Saint Etienne du Rouvray Cedex, France

Within the scope of the self-consistent-field (SCF) and mean-SCF (MSCF) approximations, static-concentration-waves and Matsubara–Kanzaki–Krivoglaz lattice statics methods, on the basis of state-of-the-art diffraction data concerning coherent and diffuse scattering of radiations in (dis)ordered f.c.c.-Ni–Fe alloys for various composition–temperature regions, and on the basis of data of independent magnetic measurements, the regular parameterization and estimation of 'pair-wise' interatomic interactions of the various nature (namely, 'direct' short-range 'electrochemical' and magnetic contributions as well as indirect long-range 'strain-induced' interaction) have been carried out taking into account their concentration and temperature dependences. As shown unfortunately, many of available 'electrochemical' interaction parameters obtained with use of the well-known *ab initio* and semi-phenomenological computational methodologies are limited in their applications for the statistical-thermodynamic analysis of f.c.c.-Ni–Fe alloys because most of them are contrary to the regularities of a 'mixing'-energy symmetry and, as a result, to the symmetries of observed $L1_2$-Ni_3Fe-, $L1_0$-NiFe- or $L1_2$-Fe_3Ni-type ordered phas-

es. The 'strain-induced' interaction energy is anisotropic, long-range and quasi-oscillating function of a distance between the solute atoms in a host crystal (throughout the temperature–concentration region of f.c.c.-Ni–Fe alloys). Combined 'paramagnetic' contribution to the 'mixing' energy depends implicitly and essentially on concentration of Fe atoms, and its minimum Fourier-component values fall in the range of Invar compositions of Ni–Fe alloy. The temperature dependence of total 'mixing' energy is mainly due to the significant temperature-dependent magnetic contribution to it, and there is no need to take into account the effects of both substitutional correlations between atoms and many-particle interatomic-force interactions for characterization of microstructures developed by atomic ordering and (or) solid-phase precipitation in f.c.c.-Ni–Fe alloys. As expected, within the scope of the MSCF approximation, the estimated energy parameters of 'exchange' interactions in 1st coordination shell, $J_{\mathrm{NiNi}}(r_1)$ and $J_{\mathrm{NiFe}}(r_1)$, correspond to the ferromagnetic interaction between magnetic moments in Ni–Ni and Ni–Fe atomic pairs, and $J_{\mathrm{FeFe}}(r_1)$ corresponds to the antiferromagnetic interaction between magnetic moments in Fe–Fe atomic pairs.

У рамках наближень самоузгодженого (СУП) та середнього самоузгодженого (ССУП) полів, метод статичних концентраційних хвиль (СКХ) і статики ґратниці Мацубари–Канзакі–Кривоглаза, на основі сучасних дифракційних даних стосовно когерентного та дифузного розсіяння випромінення у (не)впорядкованих стопах ГЦК-Ni–Fe в широкій концентраційно-температурній області, а також за даними незалежних магнетних мірянь виконано систематичну параметризацію та кількісний розрахунок енергій «парних» міжатомових взаємодій різної природи (а саме, «прямих» близькосяжних «електрохемічного» й магнетного внесків, а також непрямої далекосяжної «деформаційної» взаємодії) із врахуванням їх концентраційної і температурної залежностей. Недвозначно показано, що більшість значень параметрів «електрохемічних» взаємодій компонентів, наведених у спеціялізованій науковій літературі, яких було оцінено із застосуванням відомих «першопринципних» та напівфеноменологічних обчислювальних методологій, на жаль, не задовольняють загальним правилам симетрії енергій «змішання» (в оберненому й прямому просторах), а отже й симетрії експериментально спостережуваних фаз, атомовоупорядкованих за надструктурними типами $L1_2$-Ni_3Fe, $L1_0$-NiFe або $L1_2$-Fe_3Ni. В усій температурно-концентраційній області стопів ГЦК-Ni–Fe енергія «деформаційної» взаємодії є анізотропною, далекосяжною і квазиосцилівною функцією віддалі між домішковими атомами, розчиненими в основному ГЦК-кристалі. Спільний «парамагнетний» («електрохемічний» + «деформаційний») внесок у енергію «змішання» суттєво залежить від концентрації атомів Fe, а мінімум його Фур'є-компоненти з хвильовим вектором $\mathbf{k}_\Gamma(0\,0\,0)$ лежить в інварному інтервалі складів стопів Ni–Fe. Температурна залежність повної енергії «змішання» в основному обумовлюється суттєвою температурною залежністю її магнетної складової; тому втрачає свою розрахункову необхідність (та й фізичну доцільність) урахування ефектів багаточастинкових взаємодій і міжатомових кореляцій заміщення для аналізи мікроструктури, що розвивається через атомове впорядкування та (або) твердофазний розпад стопів ГЦК-Ni–Fe. Як і очікувалося, оцінені в рамках наближення ССУП енергетичні параметри «обмінних» взаємодій у першій координа-

ційній сфері $J_{NiNi}(r_I)$ та $J_{NiFe}(r_I)$ відповідають феромагнетному характеру взаємодій між магнетними моментами у атомових парах Ni–Ni й Ni–Fe, а $J_{FeFe}(r_I)$ — антиферомагнетному характеру взаємодії між магнетними моментами у атомових парах Fe–Fe.

В рамках приближений самосогласованного (ССП) и среднего самосогласованного (СССП) полей, методов статических концентрационных волн (СКВ) и статики решетки Мацубары–Канзаки–Кривоглаза, на основе современных дифракционных данных о когерентном и диффузном рассеяния излучений в (не)упорядоченных сплавах ГЦК-Ni–Fe в широкой концентрационно-температурной области и по данным независимых магнитных измерений проведена систематическая параметризация и количественный расчет энергий «парных» межатомных взаимодействий различной природы (а именно, «прямых» близкодействующих «электрохимического» и магнитного вкладов, а также косвенного дальнодействующего «деформационного» взаимодействия) с учетом их концентрационной и температурной зависимостей. Недвусмысленно показано, что большинство значений параметров «электрохимических» взаимодействий компонентов, приведенных в специализированной научной литературе, которые были оценены с применением известных «первопринципных» и полуфеноменологических вычислительных методологий, к сожалению, не удовлетворяют общим правилам симметрии энергий «смешения» (в обратном и прямом пространствах) и, следовательно, симметрии экспериментально обнаруженных фаз, атомноупорядоченных по сверхструктурным типам $L1_2$-Ni_3Fe, $L1_0$-NiFe или $L1_2$-Fe_3Ni. Во всей температурно-концентрационной области сплавов ГЦК-Ni–Fe энергия «деформационного» взаимодействия является анизотропной, дальнодействующей и квазиосциллирующей функцией расстояния между примесными атомами, растворенными в основном кристалле. Общий «парамагнитный» («электрохимический» + «деформационный») вклад в энергию «смешения» существенно зависит от концентрации атомов Fe, а минимум его фурье-компоненты с волновым вектором $\mathbf{k}_\Gamma(0\,0\,0)$ лежит в инварной области составов сплавов Ni–Fe. Температурная зависимость полной энергии «смешения» в основном обусловлена существенной температурной зависимостью ее магнитной слагающей; поэтому теряет свою расчетную необходимость (да и физическую целесообразность) учет эффектов многочастичных взаимодействий и межатомных корреляций замещения при анализе микроструктуры, развивающейся посредством атомного упорядочения и (или) твердофазного распада сплавов ГЦК-Ni–Fe. Как и ожидалось, оцененные в рамках приближения СССП энергетические параметры «обменных» взаимодействий в первой координационной сфере $J_{NiNi}(r_I)$ и $J_{NiFe}(r_I)$ отвечают ферромагнитному характеру взаимодействий между магнитными моментами в парах атомов Ni–Ni и Ni–Fe, а $J_{FeFe}(r_I)$ — антиферромагнитному характеру взаимодействия между магнитными моментами в парах атомов Fe–Fe.

Keywords: Ni–Fe alloys, interatomic interactions, statistical thermodynamics, order–disorder transformations, magnetic transitions, diffuse scattering.

(Received 20 September, 2010; in final version 21 November, 2010)

1. INTRODUCTION

Physical-mechanical and magnetic properties [1–24] of f.c.c.-Ni–Fe alloys have provided their wide use in a current technology as multipurpose materials. These properties significantly depend on microstructure and phase composition as well as the heat and thermomechanical treatments determining a prehistory of alloys. For instance, in the Fe-atoms' concentration region, $0.1 < c < 0.3$, so-called Permalloys are formed. These soft magnetic materials characterized by fast processes of magnetic reversal can have atomic long-range-ordered $L1_2$-Cu_3Au-type (Ni_3Fe) structure, near-zero magnetostriction and magnetic-anisotropy constants [1–5]. In a concentration region of Fe atoms, $0.45 < c < 0.55$, Elinvars are formed (with atomic long-range-ordered $L1_0$-CuAuI-type (NiFe) layered structure with temperature factor of electrical resistance possessing high values) [2]. A special attention should be paid to Fe–Ni Invars [1–3, 18–24] with relative concentration of Fe atoms close to $c \cong 0.65$. Near this chemical composition, such an alloy has microheterogeneous structure, which may be probably atomic long-range-ordered of $L1_2$-Cu_3Au type (Fe_3Ni) in part. In some temperature interval, the Invar alloy undergoes an abnormally low thermal expansion of crystal lattice. All these alloys have found a wide practical application in precise instrument making, measuring standards, *etc*. In connection with an urgency of Ni–Fe alloys, persistent experimental and theoretical investigations of their properties are being held until nowadays [1–24]. It is evident that such a wide set of physical properties of Ni–Fe alloys depending on both the composition and the temperature has the microscopic nature, in particular, spatial distributions of ions and their uncompensated magnetic moments over the sites of f.c.c. lattice, distributions of fields of the static and dynamic distortions, crystal defects, *etc*. In case of microscopically inhomogeneous atomic and (or) magnetic states' distributions (that takes place, *e.g.*, within the Invar alloy) and (or) heterogeneous phase states, the alloy properties are controlled by the spatial distributions of composition (magnetic) inhomogeneities, morphology of phases, *etc*. Certainly, all the mentioned characteristics are governed by both the generally long-range interatomic force interactions and the statistical-correlation effects for substitutional atoms in an alloy, for instance, approaching to the critical points: the order–disorder phase transformation temperature—Kurnakov's point, T_K, and magnetic phase transition temperature—Curie (or Néel) point, $T_C(T_N)$.

In a given article, developing the atomistic model of f.c.c.-Ni–Fe alloys, the quantitative estimation of interatomic-interaction energy parameters for the atomic and magnetic subsystems is proposed, including their concentration and temperature dependences and considering the magnetism of both constituents (*i.e.* Ni and Fe atoms) allowing for

the significant distinction of their uncompensated magnetic-moments' values. At the following step, we analyze an influence of both the long-range atomic order of spatial atomic configurations and the magnetism using the simplest self-consistent-field (SCF) and mean-SCF (MSCF) approximations, respectively. Thus, we assume that interatomic ('paramagnetic' and magnetic) interactions are virtually pair-wise and consist of short-range 'direct' (inherently 'electrochemical' and magnetic) contribution and long-range one (in fact, 'strain-induced', *i.e.* due to the atomic-size mismatch between Ni and Fe atoms). Based on the static concentration waves (SCW) method [25, 26], we consider quantitatively expressions for the configuration-dependent parts of free energies (Helmholtz thermodynamic potentials) for both atomic and magnetic subsystems in corresponding long-range ordered phases of $L1_2$-Ni_3Fe, $L1_0$-NiFe or $L1_2$-Fe_3Ni type. Besides, at each step of consecutive development of microscopic model of f.c.c.-Ni–Fe alloys and definition of interatomic-interaction parameterization, the results of other authors are analyzed in symmetry details.

2. STATISTICAL THERMODYNAMICS OF F.C.C. SUBSTITUTIONAL ALLOYS WITH TWO MAGNETIC CONSTITUENTS

Within the scope of the conventional statistical-thermodynamic model of a solid solution [25–30], the simplest approximation of pair-wise interatomic interaction is commonly used. Within this model, the total configuration-dependent energy of the $A_{1-c}B_c$ solid alloy in its paramagnetic state or in absence of any magnetic interatomic interactions can be presented as a sum of interaction energies of separate pairs of atoms. The configuration-dependent part of the Hamiltonian can be used [25–30]:

$$H_{\text{conf}}^{\text{at}} \approx H_{01}(c) + \frac{1}{2}\sum_{\mathbf{R}}\sum_{\mathbf{R}'} w_{\text{prm}}(\mathbf{R}-\mathbf{R}')C_{\mathbf{R}}C_{\mathbf{R}'}, \qquad (1)$$

where summation is made over all $N_{\text{u.c.}}$ radius-vectors of the Bravais lattice sites, $\{\mathbf{R}, \mathbf{R}'\}$; $C_{\mathbf{R}} = 1$, if, at the site $\mathbf{R}$, there is an alloying B atom, and $C_{\mathbf{R}} = 0$, if, at the site $\mathbf{R}$, there is a host A atom; $H_{01}(c) = O(c)$. The 'mixing' energy, $w_{\text{prm}}(\mathbf{r})$, at the radius-vector $\mathbf{r} = \mathbf{R} - \mathbf{R}'$ for A–B alloys in a paramagnetic state with zero effective local magnetic-moment values is defined as follows [25, 26, 28, 30]:

$$w_{\text{prm}}(\mathbf{r}) = W_{\text{prm}}^{AA}(\mathbf{r}) + W_{\text{prm}}^{BB}(\mathbf{r}) - 2W_{\text{prm}}^{AB}(\mathbf{r}) \qquad (2)$$

(sometimes, with the gauge of $w_{\text{prm}}(\mathbf{R}-\mathbf{R}) \equiv w_{\text{prm}}(\mathbf{0}) = 0$ as a condition of the self-action lack), where $W_{\text{prm}}^{AA}(\mathbf{r})$, $W_{\text{prm}}^{BB}(\mathbf{r})$, $W_{\text{prm}}^{AB}(\mathbf{r})$ are the pair-wise interatomic-interaction energies in A–A, B–B and A–B pairs of atoms, which are located at the sites $\mathbf{R}$ and $\mathbf{R}'$ at a distance $\mathbf{r}$ from each oth-

er, respectively. 'Paramagnetic' 'mixing' energy, $w_{\text{prm}}(\mathbf{r})$, can be separated into two contributions [25, 26]: $w_{\text{prm}}(\mathbf{r}) \cong \varphi_{\text{chem}}(\mathbf{r}) + V_{\text{si}}^{BB}(\mathbf{r})$, *i.e.* 'electrochemical' and 'strain-induced' interatomic-interaction energies. Within the SCF approximation, the configuration-dependent part of internal energy of atomic subsystem can be written as follows [25, 26]:

$$U_{\text{conf}}^{\text{at}} \cong U_{01}(c) + \frac{1}{2}\sum_{\mathbf{R}}\sum_{\mathbf{R}'} w_{\text{prm}}(\mathbf{R}-\mathbf{R}')P(\mathbf{R})P(\mathbf{R}'), \qquad (3)$$

where $P(\mathbf{R})$ is the single-site occupation-probability function representing the probability of finding a B atom at the site with the origin at $\mathbf{R}$. $U_{01}(c) = O(c)$. Within the scope of the SCF approximation, expression for the configuration-dependent part of entropy of atomic subsystem in a binary alloy is as follows [25, 26]:

$$S_{\text{conf}}^{\text{at}} \cong -k_B \sum_{\mathbf{R}} \{P(\mathbf{R})\ln P(\mathbf{R}) + \left[1-P(\mathbf{R})\right]\ln\left[1-P(\mathbf{R})\right]\}, \qquad (4)$$

where k_B is the Boltzmann constant.

As well known [25, 26], the statistical thermodynamics of an alloy is determined by the several Fourier components of interatomic-interaction energies only. These parameters, $\tilde{w}_{\text{prm}}(\mathbf{k}_\Gamma = \mathbf{0})$ and $\tilde{w}_{\text{prm}}(\mathbf{k}_1)$, ..., $\tilde{w}_{\text{prm}}(\mathbf{k}_s)$, ..., $\tilde{w}_{\text{prm}}(\mathbf{k}_{\ell-1})$, are the Fourier components of 'paramagnetic' contributions to 'mixing' energies and are defined by their inverse Fourier transform over direct space:

$$\tilde{w}_{\text{prm}}(\mathbf{k}) = \sum_{\mathbf{R}} w_{\text{prm}}(\mathbf{R}-\mathbf{R}')\exp\left\{-i\mathbf{k}\cdot(\mathbf{R}-\mathbf{R}')\right\}, \qquad (5)$$

where summation is made over all $N_{\text{u.c.}}$ radius-vectors of the Bravais lattice sites, $\{\mathbf{R}\}$. The reciprocal-space vector $\mathbf{k}_\Gamma = [2\pi/a_0](0\ 0\ 0)$ corresponds to the 'structural' ('fundamental') point (reciprocal-lattice site); a set of the reciprocal-space vectors $\{\mathbf{k}_s = (k_{sx}\ k_{sy}\ k_{sz}) \equiv [2\pi/a_0](q_{sx}\ q_{sy}\ q_{sz})\}$ corresponds to the 'superstructural' points, which are located within the irreducible region of the 1st Brillouin zone (*BZ*) and belong to the s-th quasi-wave-vector star generating the static concentration waves in an ordering alloy (with a_0—the equilibrium lattice parameter). The number of 'mixing'-energies' parameters is equal to ℓ, where ℓ is the number of non-equivalent Bravais sublattices, into which the lattice of disordered solid solution is subdivided after decreasing the temperature below the order–disorder phase transformation temperature, T_K. In case of f.c.c.-Ni–Fe alloys, these are, *e.g.*, $\tilde{w}_{\text{prm}}(\mathbf{k}_\Gamma)$ and $\tilde{w}_{\text{prm}}(\mathbf{k}_X)$, where the ordering quasi-wave vectors, $\mathbf{k}_{X_1} = 2\pi\mathbf{a}_1^* = [2\pi/a_0](1\ 0\ 0)$, $\mathbf{k}_{X_2} = 2\pi\mathbf{a}_2^* = [2\pi/a_0](0\ 1\ 0)$ and $\mathbf{k}_{X_3} = 2\pi\mathbf{a}_3^* = [2\pi/a_0](0\ 0\ 1)$, correspond to the high-symmetry (h-s) X points; $\mathbf{a}_1^*$, $\mathbf{a}_2^*$, $\mathbf{a}_3^*$ are the one-half fractions of translation vectors, $2\mathbf{a}_1^*$, $2\mathbf{a}_2^*$, $2\mathbf{a}_3^*$, along mutually perpendicular Cartesian directions [1 0 0], [0 1 0] and [0 0 1], respectively, in a reciprocal lattice with the 'fundamental'-translation vectors $\mathbf{b}_1 =$

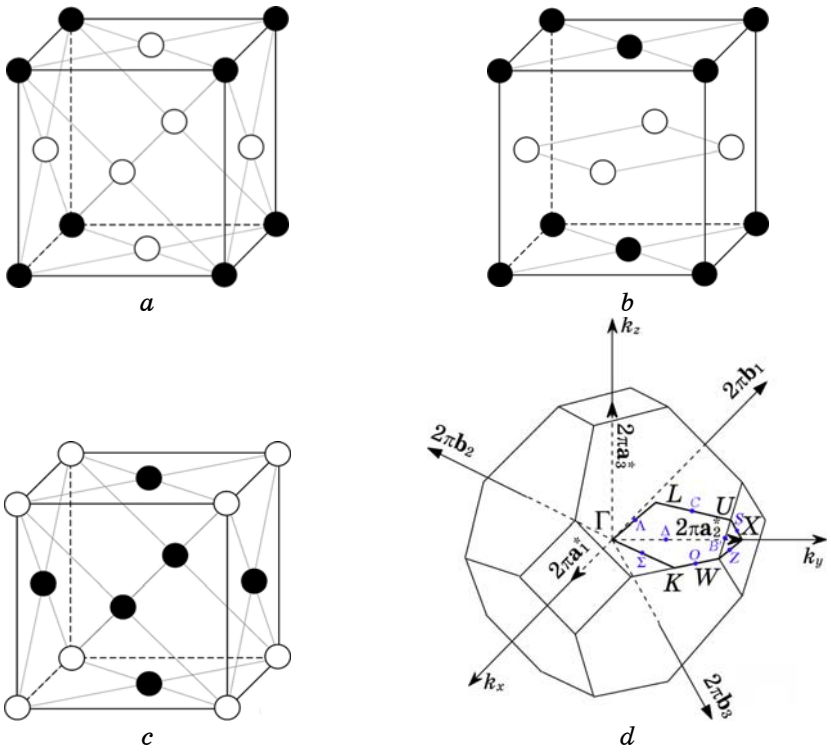

Fig. 1. Spatial arrangements of Ni (○) and Fe (●) atoms over the sites of f.c.c.-lattice conditional unit cell in perfect substitutional superstructures (with appropriate stoichiometry at $T = 0$ K): $L1_2$-type Ni_3Fe or Fe_3Ni (*a*, *c*) and $L1_0$-type NiFe (*b*). The 1st Brillouin zone of f.c.c.-lattice reciprocal space (*d*); Γ, *X*, *W*, *L*, *K*(*U*) and Δ, *Z*, *Q*, Λ, Σ, *C*, *O*, *B*′ are the h-s points and the h-s directions, respectively, within the irreducible part of the 1st *BZ* (outlined by heavy solid lines).

$= [1/a_0](-1\ 1\ 1)$, $\mathbf{b}_2 = [1/a_0](1\ -1\ 1)$ and $\mathbf{b}_3 = [1/a_0](1\ 1\ -1)$.

As known, in f.c.c.-Ni–Fe alloys, the order–disorder phase transformations are observed, and from disordered f.c.c. (*A*1-type) solid solution (with atomic short-range order (SRO) only), the $L1_2$-Cu_3Au-type or $L1_0$-CuAu*I*-type substitutional (super)structures are formed [1–24]; see Fig. 1, *a*–*c*. The 1st *BZ* and its irreducible part are also shown in Fig. 1, *d*.

The $L1_2$-Cu_3Au-type structure is characterized by the following distribution of probabilities of substituting the f.c.c.-lattice sites with alloying-constituent atoms [25, 26]:

$$P(\mathbf{R}) = c + \frac{\eta}{4}\left[\exp\left(i2\pi\mathbf{a}_1^* \cdot \mathbf{R}\right) + \exp\left(i2\pi\mathbf{a}_2^* \cdot \mathbf{R}\right) + \exp\left(i2\pi\mathbf{a}_3^* \cdot \mathbf{R}\right)\right], \quad (6)$$

and for the $L1_0$-CuAu*I*-type structure, the probability distribution is as follows [25, 26]:

$$P(\mathbf{R}) = c + \frac{\eta}{2}\exp\left(i2\pi\mathbf{a}_1^* \cdot \mathbf{R}\right), \tag{7}$$

where c is the relative concentration of alloying B atoms in f.c.c. host crystal of A atoms, η is an appropriate atomic long-range order (LRO) parameter.

Substituting these distribution functions (6), (7) into expressions for configuration-dependent part of internal energy (3), and entropy for atomic subsystem of an alloy (4), we obtain [25, 26]:

$$U_{\text{conf}}^{\text{at}} \cong U_{01}(c) + \frac{N_{\text{u.c.}}}{2}\left\{\tilde{w}_{\text{prm}}(\mathbf{0})c^2 + \frac{3\eta^2}{16}\tilde{w}_{\text{prm}}(\mathbf{k}_X)\right\}, \tag{8}$$

$$S_{\text{conf}}^{\text{at}}(\eta) \cong -\frac{k_B N_{\text{u.c.}}}{4}\left\{3\left(c-\frac{\eta}{4}\right)\ln\left(c-\frac{\eta}{4}\right) + 3\left(1-c+\frac{\eta}{4}\right)\ln\left(1-c+\frac{\eta}{4}\right) + \right.$$

$$\left. + \left(c+\frac{3\eta}{4}\right)\ln\left(c+\frac{3\eta}{4}\right) + \left(1-c-\frac{3\eta}{4}\right)\ln\left(1-c-\frac{3\eta}{4}\right)\right\} \tag{9}$$

for the $L1_2$-Ni_3Fe-type structure (or the $L1_2$-Fe_3Ni-type one with replacement of c by $1-c$), and

$$U_{\text{conf}}^{\text{at}} \cong U_{01}(c) + \frac{N_{\text{u.c.}}}{2}\left\{\tilde{w}_{\text{prm}}(\mathbf{0})c^2 + \frac{\eta^2}{4}\tilde{w}_{\text{prm}}(\mathbf{k}_X)\right\}, \tag{10}$$

$$S_{\text{conf}}^{\text{at}}(\eta) \cong -\frac{k_B N_{\text{u.c.}}}{2}\left\{\left(1-c-\frac{\eta}{2}\right)\ln\left(1-c-\frac{\eta}{2}\right) + \left(c+\frac{\eta}{2}\right)\ln\left(c+\frac{\eta}{2}\right) + \right.$$

$$\left. + \left(1-c+\frac{\eta}{2}\right)\ln\left(1-c+\frac{\eta}{2}\right) + \left(c-\frac{\eta}{2}\right)\ln\left(c-\frac{\eta}{2}\right)\right\} \tag{11}$$

for the $L1_0$-NiFe-type structure.

In Equations (8), (10), the quasi-wave vector $\mathbf{k}_X$ describes both the $L1_2$-type structures in Permalloys or Invars and the $L1_0$-type structure in Elinvars.

Thus, the total configuration-dependent part of free energy for atomic subsystem in a paramagnetic state of an alloy is defined by the conventional relation [25–30]: $F_{\text{conf}}^{\text{at}} = U_{\text{conf}}^{\text{at}} - TS_{\text{conf}}^{\text{at}}$.

An occurrence of magnetism in f.c.c.-Ni–Fe alloys (with both magnetic constituents having atomic spin numbers s_{Ni} and s_{Fe}) complicates appreciably the analysis of their statistical thermodynamics [1–24, 31–38]. Within the scope of the molecular-field (MF, *i.e.* MSCF) approximation, the configuration-dependent part of internal energy for magnetic subsystem is defined as follows [36, 37]:

$$U_{\text{conf}}^{\text{mag}} \cong \frac{N_{\text{u.c.}}}{2}\Big\{\tilde{J}_{\text{NiNi}}(\mathbf{0})\, s_{\text{Ni}}^2 (1-c)^2 \sigma_{\text{Ni}}^2 + \tilde{J}_{\text{FeFe}}(\mathbf{0})\, s_{\text{Fe}}^2 c^2 \sigma_{\text{Fe}}^2 +$$

$$+2\tilde{J}_{\text{NiFe}}(\mathbf{0})\, s_{\text{Ni}} s_{\text{Fe}} (1-c) c \sigma_{\text{Ni}} \sigma_{\text{Fe}} +$$

$$+\frac{3\eta^2}{16}\Big[\tilde{J}_{\text{NiNi}}(\mathbf{k}_X)\, s_{\text{Ni}}^2 \sigma_{\text{Ni}}^2 + \tilde{J}_{\text{FeFe}}(\mathbf{k}_X)\, s_{\text{Fe}}^2 \sigma_{\text{Fe}}^2 - 2\tilde{J}_{\text{NiFe}}(\mathbf{k}_X)\, s_{\text{Ni}} s_{\text{Fe}} \sigma_{\text{Ni}} \sigma_{\text{Fe}}\Big]\Big\} \quad (12)$$

for the $L1_2$-Ni_3Fe-type structure (or, with replacement of subscripts '$_{Fe}$' by subscripts '$_{Ni}$', for the $L1_2$-Fe_3Ni-type one), and

$$U_{\text{conf}}^{\text{mag}} \cong \frac{N_{\text{u.c.}}}{2}\Big\{\tilde{J}_{\text{NiNi}}(\mathbf{0})\, s_{\text{Ni}}^2 (1-c)^2 \sigma_{\text{Ni}}^2 + \tilde{J}_{\text{FeFe}}(\mathbf{0})\, s_{\text{Fe}}^2 c^2 \sigma_{\text{Fe}}^2 +$$

$$+2\tilde{J}_{\text{NiFe}}(\mathbf{0})\, s_{\text{Ni}} s_{\text{Fe}} (1-c) c \sigma_{\text{Ni}} \sigma_{\text{Fe}} +$$

$$+\frac{\eta^2}{4}\Big[\tilde{J}_{\text{NiNi}}(\mathbf{k}_X)\, s_{\text{Ni}}^2 \sigma_{\text{Ni}}^2 + \tilde{J}_{\text{FeFe}}(\mathbf{k}_X)\, s_{\text{Fe}}^2 \sigma_{\text{Fe}}^2 - 2\tilde{J}_{\text{NiFe}}(\mathbf{k}_X)\, s_{\text{Ni}} s_{\text{Fe}} \sigma_{\text{Ni}} \sigma_{\text{Fe}}\Big]\Big\} \quad (13)$$

for the $L1_0$-NiFe-type structure. In Equations (12), (13), the relationship between the Fourier components of 'exchange' 'integrals' for magnetic interactions and their Fourier transforms is as follows:

$$\tilde{J}_{\alpha\alpha'}(\mathbf{k}) = \sum_{\mathbf{R}} J_{\alpha\alpha'}(\mathbf{R}-\mathbf{R}')\, e^{-i\mathbf{k}\cdot(\mathbf{R}-\mathbf{R}')}\,. \quad (14)$$

Here, summation is made over all radius-vectors, $\{\mathbf{R}\}$, of sites relating to coordination shells around the site $\mathbf{R}'$ within the Bravais lattice. $J_{\alpha\alpha'}(\mathbf{R}-\mathbf{R}')$ are the 'exchange' 'integrals' for magnetic interactions between the uncompensated magnetic moments of atoms (α, α' = Ni, Fe), which are located at the sites $\mathbf{R}$ and $\mathbf{R}'$ (at that, $J_{\alpha\alpha'}(\mathbf{R}-\mathbf{R}') = J_{\alpha'\alpha}(\mathbf{R}'-\mathbf{R}) = J_{\alpha'\alpha}(\mathbf{R}-\mathbf{R}')$); σ_{Ni} and σ_{Fe} are the average spontaneous magnetizations of Ni and Fe subsystems (per atom), respectively. The total 'mixing'-energy Fourier component for any quasi-wave vector in reciprocal space is defined as [36, 37]

$$\tilde{w}_{\text{tot}}(\mathbf{k}) \approx \tilde{w}_{\text{prm}}(\mathbf{k}) + \tilde{w}_{\text{mag}}(\mathbf{k}) \cong \tilde{\varphi}_{\text{chem}}(\mathbf{k}) + \tilde{V}_{\text{si}}^{\alpha'\alpha'}(\mathbf{k}) + \tilde{w}_{\text{mag}}(\mathbf{k}) \cong$$

$$\cong \tilde{\varphi}_{\text{chem}}(\mathbf{k}) + \tilde{V}_{\text{si}}^{\alpha'\alpha'}(\mathbf{k}) + \tilde{J}_{\text{NiNi}}(\mathbf{k})\, s_{\text{Ni}}^2 \sigma_{\text{Ni}}^2 +$$

$$+\tilde{J}_{\text{FeFe}}(\mathbf{k})\, s_{\text{Fe}}^2 \sigma_{\text{Fe}}^2 - 2\tilde{J}_{\text{NiFe}}(\mathbf{k})\, s_{\text{Ni}} s_{\text{Fe}} \sigma_{\text{Ni}} \sigma_{\text{Fe}} \quad (15)$$

for α–α' alloy with α' = Fe, Ni if α = Ni, Fe, respectively. Here, the 'mixing'-energy Fourier component for such an alloy in a paramagnetic state, $\tilde{w}_{\text{prm}}(\mathbf{k})$, is presented in the form of a sum of two contributions: 'direct' contribution of short-range and isotropic 'electrochemi-

cal' interactions, $\tilde{\varphi}_{\text{chem}}(\mathbf{k})$, and indirect contribution of anisotropic, long-range and 'quasi-oscillating' 'strain-induced' interaction, $\tilde{V}_{\text{si}}^{\alpha'\alpha'}(\mathbf{k})$, arising between the dissolved α' atoms (α' = Fe (Ni)) in a host crystal consisting of α atoms (α = Ni (Fe)) (see details below). Generally (and especially, for transition-metal alloys), 'paramagnetic' 'mixing'-energy Fourier component contains one more indirect long-range electron–electron-interaction-mediated contribution, $\tilde{w}_{\text{el}}(\mathbf{k})$. This contribution arises when the ordering quasi-wave vector magnitude is nearly equal to the Fermi-surface diameter, $|\mathbf{k}_s| \approx 2k_F$ or $|\mathbf{k}_s + 2\pi\mathbf{b}| \approx 2k_F$ ($\mathbf{b}$ is the Bragg ('structural') 'fundamental' vector of reciprocal lattice), and $\mathbf{k}_s$ coincides with Fermi-surface flat, elliptic or cylindrical regions [30]. Unlike 'strain-induced' interaction, forces of indirect 'electron–electron'-interaction-mediated contribution manifest themselves first and foremost at $\mathbf{k} \to \mathbf{k}_s \neq \mathbf{0}$ (but not at $\mathbf{k} \to \mathbf{0}$) that leads to occurrence of global minima of the $\tilde{w}_{\text{tot}}(\mathbf{k})$ function for quasi-wave vectors, which are distinct from 'superstructural' h-s points on the 1st *BZ* surface, $\min\limits_{\mathbf{k}\in BZ} \tilde{w}_{\text{tot}}(\mathbf{k}) \neq \tilde{w}_{\text{tot}}(\mathbf{k}_s)$ (where $\mathbf{k}_s = \mathbf{k}_X$, $\mathbf{k}_W$, $\mathbf{k}_{K(U)}$ or $\mathbf{k}_L$ for f.c.c.-lattice reciprocal space; see Fig. 1, *d*), that leads by-turn to the splitting of radiation diffuse scattering intensity, $I_{\text{SRO}}(\mathbf{k})$, in the vicinity of a 'superstructural' point with $\mathbf{k} = \mathbf{k}_s$. Thus, the long-period structures with atomic LRO (*i.e.* inhomogeneous structures with spatially changing values of atomic-LRO parameter and composition) become thermodynamically favourable. There are certain examples of such alloys: Cu–Pd, Cu–Al, Cu–Au, *etc.* [30]. Concerning theoretical description of such a phenomena, see articles of Tsatskis referred below in section 3 and references therein.

Taking into account magnetism of an alloy, the total configuration-dependent part of free energy can be written as follows [36, 37]:

$$F_{\text{conf}} = U_{\text{conf}} - TS_{\text{conf}} = U_{\text{conf}}^{\text{at}} + U_{\text{conf}}^{\text{mag}} - T\left(S_{\text{conf}}^{\text{at}} + \sum_{\alpha=\text{Ni,Fe}} S_{\text{conf}}^{\text{mag}(\alpha)}\right). \quad (16)$$

Statistical-thermodynamic calculation of the magnetic entropy, $S_{\text{conf}}^{\text{mag}(\alpha)}$, for each α-th subsystem of atomic magnetic moments appears more complicated. For the cases only when the spin-number values are equal to 1/2 [31–33, 35], 1 [34, 35], 3/2 [35] and 2 [35], the explicit expressions for magnetic entropy have been obtained by the steepest descent method. Hereinafter, we use the implicit expression for configurational magnetic entropy for any integer or half-integer spin numbers, *e.g.*, s_α = 1/2, 1, 3/2, 2, 5/2, obtained within the scope of the MF (*i.e.* MSCF) approximation [38] and presented in Refs. [36, 37]:

$$S_{\text{conf}}^{\text{mag}(\alpha)} \cong N_{\text{u.c.}} k_B c_\alpha \left[\ln \text{sh} \left(\left(1 + \frac{1}{2s_\alpha} \right) y_\alpha \right) - \ln \text{sh} \left(\frac{1}{2s_\alpha} y_\alpha \right) - y_\alpha \beta_{s_\alpha} (y_\alpha) \right] \quad (17)$$

($\alpha = \text{Ni, Fe}$), where $c_{\text{Fe}} = c$, $c_{\text{Ni}} = 1 - c$, and the well-known Brillouin function, $\beta_{s_\alpha}(y_\alpha)$, is defined as follows [38]:

$$\beta_{s_\alpha}(y_\alpha) = \left(1 + \frac{1}{2s_\alpha} \right) \text{cth} \left[\left(1 + \frac{1}{2s_\alpha} \right) y_\alpha \right] - \frac{1}{2s_\alpha} \text{cth} \left(\frac{1}{2s_\alpha} y_\alpha \right) (\alpha = \text{Ni, Fe}). \quad (18)$$

Here, $y_\alpha = (s_\alpha H_{\text{eff}}^\alpha)/(k_B T)$ is the characteristic magnetic-interaction-to-thermal-fluctuation-energy ratio in the effective internal magnetic mean field, $H_{\text{eff}}^\alpha \cong -g\mu_B \Sigma_{\alpha' = \text{Ni, Fe}} \Gamma_{\alpha\alpha'} \sigma_{\alpha'}$; g is the Landé factor ($g \cong 2$); μ_B is the Bohr magneton; $\{\Gamma_{\alpha\alpha'}\}$ are the Weiss 'molecular-field' coefficients; $\sigma_{\alpha'}$ is the relative average spontaneous magnetization (in units of $s_{\alpha'} g \mu_B$) of α'-th magnetic subsystem (per atom); $\alpha, \alpha' = \text{Ni, Fe}$.

Substituting Equations (8)–(11), (12), (13), (17) into (16), we obtain the following expressions for the total configuration-dependent part of free energy for magnetic alloy with atomic LRO [36, 37]:

$$\frac{F_{\text{conf}}}{N_{\text{u.c.}}} \cong \frac{1}{2} \Big[\tilde{w}_{\text{prm}}(\mathbf{0}) c^2 + \tilde{J}_{\text{NiNi}}(\mathbf{0}) s_{\text{Ni}}^2 (1-c)^2 \sigma_{\text{Ni}}^2 +$$

$$+ 2\tilde{J}_{\text{NiFe}}(\mathbf{0}) s_{\text{Ni}} s_{\text{Fe}} (1-c) c \sigma_{\text{Ni}} \sigma_{\text{Fe}} + \tilde{J}_{\text{FeFe}}(\mathbf{0}) s_{\text{Fe}}^2 c^2 \sigma_{\text{Fe}}^2 +$$

$$+ \frac{3\eta^2}{16} \Big(\tilde{w}_{\text{prm}}(\mathbf{k}_X) + \tilde{J}_{\text{NiNi}}(\mathbf{k}_X) s_{\text{Ni}}^2 \sigma_{\text{Ni}}^2 + \tilde{J}_{\text{FeFe}}(\mathbf{k}_X) s_{\text{Fe}}^2 \sigma_{\text{Fe}}^2 -$$

$$- 2\tilde{J}_{\text{NiFe}}(\mathbf{k}_X) s_{\text{Ni}} s_{\text{Fe}} \sigma_{\text{Ni}} \sigma_{\text{Fe}} \Big) \Big] + \frac{U_{01}(c)}{N_{\text{u.c.}}} +$$

$$+ \frac{k_B T}{4} \left[3 \left(c - \frac{\eta}{4} \right) \ln \left(c - \frac{\eta}{4} \right) + 3 \left(1 - c + \frac{\eta}{4} \right) \ln \left(1 - c + \frac{\eta}{4} \right) + \right.$$

$$\left. + \left(c + \frac{3\eta}{4} \right) \ln \left(c + \frac{3\eta}{4} \right) + \left(1 - c - \frac{3\eta}{4} \right) \ln \left(1 - c - \frac{3\eta}{4} \right) \right] -$$

$$- k_B T (1-c) \left[\ln \text{sh} \left(\left(1 + \frac{1}{2s_{\text{Ni}}} \right) y_{\text{Ni}} (\sigma_{\text{Ni}}, \sigma_{\text{Fe}}) \right) - \right.$$

$$\left. - \ln \text{sh} \left(\frac{1}{2s_{\text{Ni}}} y_{\text{Ni}} (\sigma_{\text{Ni}}, \sigma_{\text{Fe}}) \right) - \sigma_{\text{Ni}} y_{\text{Ni}} (\sigma_{\text{Ni}}, \sigma_{\text{Fe}}) \right] -$$

$$-k_BTc\left[\ln\mathrm{sh}\left(\left(1+\frac{1}{2s_{\mathrm{Fe}}}\right)y_{\mathrm{Fe}}\left(\sigma_{\mathrm{Fe}},\sigma_{\mathrm{Ni}}\right)\right)-\right.$$

$$\left.-\ln\mathrm{sh}\left(\frac{1}{2s_{\mathrm{Fe}}}y_{\mathrm{Fe}}\left(\sigma_{\mathrm{Fe}},\sigma_{\mathrm{Ni}}\right)\right)-\sigma_{\mathrm{Fe}}y_{\mathrm{Fe}}\left(\sigma_{\mathrm{Fe}},\sigma_{\mathrm{Ni}}\right)\right] \qquad (19)$$

for the $L1_2$-Ni_3Fe-type structure or, with trivial replacement of subscripts, the $L1_2$-Fe_3Ni-type one;

$$\frac{F_{\mathrm{conf}}}{N_{\mathrm{u.c.}}}\cong\frac{1}{2}\left[\tilde{w}_{\mathrm{prm}}\left(\mathbf{0}\right)c^2+\tilde{J}_{\mathrm{NiNi}}\left(\mathbf{0}\right)s_{\mathrm{Ni}}^2\left(1-c\right)^2\sigma_{\mathrm{Ni}}^2+\right.$$

$$+2\tilde{J}_{\mathrm{NiFe}}\left(\mathbf{0}\right)s_{\mathrm{Ni}}s_{\mathrm{Fe}}\left(1-c\right)c\sigma_{\mathrm{Ni}}\sigma_{\mathrm{Fe}}+\tilde{J}_{\mathrm{FeFe}}\left(\mathbf{0}\right)s_{\mathrm{Fe}}^2c^2\sigma_{\mathrm{Fe}}^2+$$

$$+\frac{\eta^2}{4}\left(\tilde{w}_{\mathrm{prm}}\left(\mathbf{k}_X\right)+\tilde{J}_{\mathrm{NiNi}}\left(\mathbf{k}_X\right)s_{\mathrm{Ni}}^2\sigma_{\mathrm{Ni}}^2+\tilde{J}_{\mathrm{FeFe}}\left(\mathbf{k}_X\right)s_{\mathrm{Fe}}^2\sigma_{\mathrm{Fe}}^2-\right.$$

$$\left.\left.-2\tilde{J}_{\mathrm{NiFe}}\left(\mathbf{k}_X\right)s_{\mathrm{Ni}}s_{\mathrm{Fe}}\sigma_{\mathrm{Ni}}\sigma_{\mathrm{Fe}}\right)\right]+\frac{U_{01}\left(c\right)}{N_{\mathrm{u.c.}}}+$$

$$+\frac{k_BT}{2}\left[\left(c-\frac{\eta}{2}\right)\ln\left(c-\frac{\eta}{2}\right)+\left(1-c+\frac{\eta}{2}\right)\ln\left(1-c+\frac{\eta}{2}\right)+\right.$$

$$\left.+\left(c+\frac{\eta}{2}\right)\ln\left(c+\frac{\eta}{2}\right)+\left(1-c-\frac{\eta}{2}\right)\ln\left(1-c-\frac{\eta}{2}\right)\right]-$$

$$-k_BT\left(1-c\right)\left[\ln\mathrm{sh}\left(\left(1+\frac{1}{2s_{\mathrm{Ni}}}\right)y_{\mathrm{Ni}}\left(\sigma_{\mathrm{Ni}},\sigma_{\mathrm{Fe}}\right)\right)-\right.$$

$$\left.-\ln\mathrm{sh}\left(\frac{1}{2s_{\mathrm{Ni}}}y_{\mathrm{Ni}}\left(\sigma_{\mathrm{Ni}},\sigma_{\mathrm{Fe}}\right)\right)-\sigma_{\mathrm{Ni}}y_{\mathrm{Ni}}\left(\sigma_{\mathrm{Ni}},\sigma_{\mathrm{Fe}}\right)\right]-$$

$$-k_BTc\left[\ln\mathrm{sh}\left(\left(1+\frac{1}{2s_{\mathrm{Fe}}}\right)y_{\mathrm{Fe}}\left(\sigma_{\mathrm{Fe}},\sigma_{\mathrm{Ni}}\right)\right)-\right.$$

$$\left.-\ln\mathrm{sh}\left(\frac{1}{2s_{\mathrm{Fe}}}y_{\mathrm{Fe}}\left(\sigma_{\mathrm{Fe}},\sigma_{\mathrm{Ni}}\right)\right)-\sigma_{\mathrm{Fe}}y_{\mathrm{Fe}}\left(\sigma_{\mathrm{Fe}},\sigma_{\mathrm{Ni}}\right)\right] \qquad (20)$$

for the $L1_0$-NiFe-type structure. From Equations (19), (20), specifying the condition of zeroing first derivatives of total configuration-dependent part of free energy, $\partial F_{\mathrm{conf}}/\partial\eta$, $\partial F_{\mathrm{conf}}/\partial\sigma_{\mathrm{Fe}}$, $\partial F_{\mathrm{conf}}/\partial\sigma_{\mathrm{Ni}}$, for thermody-

namic equilibrium state, we have a set of three transcendental equations for estimation of the equilibrium values of state parameters, $\eta(T, c)$, $\sigma_{Ni}(T, c)$, $\sigma_{Fe}(T, c)$, for the atomic and magnetic subsystems [36, 37]:

$$\ln \frac{\left(c - \frac{\eta}{4}\right)\left(1 - c - \frac{3\eta}{4}\right)}{\left(c + \frac{3\eta}{4}\right)\left(1 - c + \frac{\eta}{4}\right)} \cong$$

$$\cong \frac{\eta\left[\tilde{w}_{\text{prm}}(\mathbf{k}_X) + \tilde{J}_{\text{NiNi}}(\mathbf{k}_X) s_{\text{Ni}}^2 \sigma_{\text{Ni}}^2 + \tilde{J}_{\text{FeFe}}(\mathbf{k}_X) s_{\text{Fe}}^2 \sigma_{\text{Fe}}^2 - 2\tilde{J}_{\text{NiFe}}(\mathbf{k}_X) s_{\text{Ni}} s_{\text{Fe}} \sigma_{\text{Ni}} \sigma_{\text{Fe}}\right]}{k_B T},$$

$$\sigma_{\text{Ni}} \cong \beta_{s_{\text{Ni}}}\left(-\frac{1}{(1-c)k_B T}\left\{\tilde{J}_{\text{NiNi}}(\mathbf{0}) s_{\text{Ni}}^2 (1-c)^2 \sigma_{\text{Ni}} + \tilde{J}_{\text{NiFe}}(\mathbf{0}) s_{\text{Ni}} s_{\text{Fe}} (1-c) c \sigma_{\text{Fe}} + \right.\right.$$

$$\left.\left. + \frac{3\eta^2}{16}\left[\tilde{J}_{\text{NiNi}}(\mathbf{k}_X) s_{\text{Ni}}^2 \sigma_{\text{Ni}} - \tilde{J}_{\text{NiFe}}(\mathbf{k}_X) s_{\text{Ni}} s_{\text{Fe}} \sigma_{\text{Fe}}\right]\right\}\right), \qquad (21)$$

$$\sigma_{\text{Fe}} \cong \beta_{s_{\text{Fe}}}\left(-\frac{1}{c k_B T}\left\{\tilde{J}_{\text{FeFe}}(\mathbf{0}) s_{\text{Fe}}^2 c^2 \sigma_{\text{Fe}} + \tilde{J}_{\text{NiFe}}(\mathbf{0}) s_{\text{Ni}} s_{\text{Fe}} (1-c) c \sigma_{\text{Ni}} + \right.\right.$$

$$\left.\left. + \frac{3\eta^2}{16}\left[\tilde{J}_{\text{FeFe}}(\mathbf{k}_X) s_{\text{Fe}}^2 \sigma_{\text{Fe}} - \tilde{J}_{\text{NiFe}}(\mathbf{k}_X) s_{\text{Ni}} s_{\text{Fe}} \sigma_{\text{Ni}}\right]\right\}\right)$$

for the $L1_2$-Ni_3Fe-type structure (or, with trivial replacement of subscripts '$_{Fe}$' by subscripts '$_{Ni}$', for the $L1_2$-Fe_3Ni-type one), and

$$\ln \frac{\left(c - \frac{\eta}{2}\right)\left(1 - c - \frac{\eta}{2}\right)}{\left(c + \frac{\eta}{2}\right)\left(1 - c + \frac{\eta}{2}\right)} \cong$$

$$\cong \frac{\eta\left[\tilde{w}_{\text{prm}}(\mathbf{k}_X) + \tilde{J}_{\text{NiNi}}(\mathbf{k}_X) s_{\text{Ni}}^2 \sigma_{\text{Ni}}^2 + \tilde{J}_{\text{FeFe}}(\mathbf{k}_X) s_{\text{Fe}}^2 \sigma_{\text{Fe}}^2 - 2\tilde{J}_{\text{NiFe}}(\mathbf{k}_X) s_{\text{Ni}} s_{\text{Fe}} \sigma_{\text{Ni}} \sigma_{\text{Fe}}\right]}{k_B T},$$

$$\sigma_{\text{Ni}} \cong \beta_{s_{\text{Ni}}}\left(-\frac{1}{(1-c)k_B T}\left\{\tilde{J}_{\text{NiNi}}(\mathbf{0}) s_{\text{Ni}}^2 (1-c)^2 \sigma_{\text{Ni}} + \tilde{J}_{\text{NiFe}}(\mathbf{0}) s_{\text{Ni}} s_{\text{Fe}} (1-c) c \sigma_{\text{Fe}} + \right.\right.$$

$$\left.\left. + \frac{\eta^2}{4}\left[\tilde{J}_{\text{NiNi}}(\mathbf{k}_X) s_{\text{Ni}}^2 \sigma_{\text{Ni}} - \tilde{J}_{\text{NiFe}}(\mathbf{k}_X) s_{\text{Ni}} s_{\text{Fe}} \sigma_{\text{Fe}}\right]\right\}\right), \qquad (22)$$

$$\sigma_{\mathrm{Fe}} \cong \beta_{s_{\mathrm{Fe}}} \left(-\frac{1}{ck_BT} \left\{ \tilde{J}_{\mathrm{FeFe}}(\mathbf{0}) s_{\mathrm{Fe}}^2 c^2 \sigma_{\mathrm{Fe}} + \tilde{J}_{\mathrm{NiFe}}(\mathbf{0}) s_{\mathrm{Ni}} s_{\mathrm{Fe}} (1-c) c \sigma_{\mathrm{Ni}} + \right. \right.$$

$$\left. \left. + \frac{\eta^2}{4} \left[\tilde{J}_{\mathrm{FeFe}}(\mathbf{k}_X) s_{\mathrm{Fe}}^2 \sigma_{\mathrm{Fe}} - \tilde{J}_{\mathrm{NiFe}}(\mathbf{k}_X) s_{\mathrm{Ni}} s_{\mathrm{Fe}} \sigma_{\mathrm{Ni}} \right] \right\} \right)$$

for the $L1_0$-NiFe-type structure.

Thus, knowing the Fourier components of the 'paramagnetic' interatomic-interaction and magnetic ('exchange') energy parameters, $\tilde{w}_{\mathrm{prm}}(\mathbf{k}_X)$, $\tilde{w}_{\mathrm{prm}}(\mathbf{0})$ and $\tilde{J}_{\alpha\alpha'}(\mathbf{k}_X)$, $\tilde{J}_{\alpha\alpha'}(\mathbf{0})$ (α, α' = Ni, Fe), respectively, entering in Eqs. (19)–(22), and their implicit temperature-concentration dependences, it is possible to calculate equilibrium order parameters, $\eta(T, c)$, $\sigma_{\mathrm{Ni}}(T, c)$, $\sigma_{\mathrm{Fe}}(T, c)$, and critical points, $T_C(c)$, $T_K(c)$, as functions of temperature and/or composition for Ni–Fe alloy based on the f.c.c. lattice, and to plot the equilibrium phase diagram within the whole T–c-region of occurrence of such a binary alloy subjected to atomic LRO of $L1_2$- or $L1_0$-types as well as magnetic order.

3. INTERATOMIC INTERACTIONS IN (PARA)MAGNETIC F.C.C.-Ni–Fe ALLOYS

As well known, the interatomic interactions in alloys have the crucial part during formation of their equilibrium and kinetic properties on microscopic and macroscopic scales. There are number of various statistical-thermodynamic theories and approximations for definition of such interactions in alloys. In particular, we would like to indicate on: conventional SCF approximation based on the Krivoglaz–Clapp–Moss (KCM) formula [39–42], inverse Monte Carlo (IMC) method [43], spherical model (SM) [39, 41, 42, 44, 45], Onsager cavity field (OCF) approach [46–48], Tahir-Kheli approximation [49], Vaks–Zein–Kamyshenko cluster-field (CF) approach [50–52] and cluster variation methods (CVM) [53–56], Tokar–Masanskii–Grishchenko approach based on the 'gamma' expansion method [57], alpha-expansion (AE), including high-temperature expansion methods (HTM) [58], so-called 'ring' approximation [59], and some approximations developed in works reported in [60–63]. All above-mentioned approximations can be divided into two groups: (i) reciprocal-space (**k**-space) representations [39–42, 44–49, 59–63], which have no limitation on the effective radius of interatomic interactions and (ii) direct-space (**r**-space) representations [43, 50–58] having limitations for the interatomic-interaction extent (with using a limited number of the SRO parameters, $\alpha(\mathbf{r}_{lmn})$; $l\,m\,n$— site indices on coordination shells).

Conditionally, by the physical origin of interatomic interactions and their extent in alloys, there are two kinds of atom–atom (ion–ion) inter-

actions: short-range 'direct' ('electrochemical' and magnetic) and long-range indirect (for instance, 'strain-induced') interactions. 'Electrochemical' contribution is usually understood as interatomic interaction between the atoms distributed at sites of geometrically ideal (unrelaxed or rigid!) lattice. Magnetic interaction is characterized by the 'exchange' interaction arising between the uncompensated localized magnetic moments of atoms or (and) 'quasi-free' electrons in an alloy. The atomic-size mismatch of substitutional (or interstitial) impurity atom and host-crystal one in a solid solution cause the 'strain-induced' interaction between the impurity atoms. (Inherently, for instance, 'strain-induced' (indirect) interactions in impurity Fe–Fe atomic pairs within the host Ni crystal is a result of direct ('electrochemical' and magnetic) Fe–Ni and Ni–Ni interactions in total in given lattice.) Even for impurities in cubic crystals, its position-dependent energy is anisotropic, long-range and sign-alternating spatially non-periodic ('quasi-oscillating') function of interatomic distances. The sum of these contributions gives the total 'mixing' energy of an alloy (see Eq. (15)), which is implicitly dependent on temperature and concentration. Below, within the simplest approximation, namely, considering effectively 'pair-wise' interatomic interactions only and neglecting many-particle correlation effects between substitutional atoms, we will determine the concentration-temperature dependences of these energy contributions for f.c.c.-Ni–Fe alloys.

3.1. Magnetic ('Exchange') Interatomic-Interaction Energies for F.C.C.-Ni–Fe Alloys

Many theoretical investigations [15–24, 64–81] have been devoted to studies of effects of ferro- and (or) antiferromagnetic order in alloys with atomic LRO (SRO). Conditionally, all these theories and models can be divided into two groups: (i) models, which are based on the primary contribution of itinerant electron magnetism [64, 75, 76] to magnetism of an alloy, and (ii) so-called local magnetic moment model [66–68], which implies the carriers of uncompensated magnetic moments as atoms located at the effectively-periodic lattice sites. As for magnetism of f.c.c.-Ni–Fe alloys, the basic complexity for developing such quantitative model is the simultaneous quantification of, firstly, the magnetism of both constituents of an alloy (Ni and Fe), secondly, the significant difference between Ni and Fe magnetic moments, and, thirdly, the availability of two magnetic states of Fe atoms, namely, two so-called Weiss γ-states [18–24, 66], namely, the low-spin (LS) and high-spin (HS) states. There are some methods and approaches for definition of 'exchange' 'integrals' for magnetic interactions in alloys, in particular, MSCF (or MF) approximations [69–74, 77], cluster methods in the mean-field theory [79], Monte Carlo Ising-type approximation [80], *ab initio* models [18–24, 75, 76], *etc.*

In a given article, we will use the results obtained within the scope of the MSCF approximation. Linearizing the sets of Eqs. (21), (22) with respect to σ_{Fe} and σ_{Ni}, expanding the Brillouin function (18) in Taylor series for small y_α,

$$\sigma_\alpha \approx \frac{s_\alpha + 1}{3s_\alpha}\left[y_\alpha + O\left(y_\alpha^3\right)\right], \tag{23}$$

and considering an approximate relationship as follows:

$$\tilde{J}_{\alpha\alpha'}\left(\mathbf{k}_X \text{ or } \mathbf{k}_W\right) \cong -\tilde{J}_{\alpha\alpha'}\left(\mathbf{0}\right)/3 \ (\alpha, \alpha' = \text{Fe, Ni}), \tag{24}$$

which is faithfully valid for neighbouring magnetic moments interacting within the 1st coordination shell only, if $J_{\alpha\alpha'}\left(r_{\text{I}}\right) \neq 0$, $J_{\alpha\alpha'}\left(r_{\text{II}}\right) = J_{\alpha\alpha'}\left(r_{\text{III}}\right) = \ldots = 0$, one can obtain the expression connecting the Curie temperature of magnetic phase transition with pair-wise 'exchange'-interaction parameters, composition and atomic-LRO parameters of f.c.c.-Ni–Fe alloy in a macroscopically homogeneous state [36, 37]:

$$\begin{aligned} T_C \cong -\frac{1}{6k_B}\Big\{ & \left(1+s_{\text{Ni}}\right)s_{\text{Ni}}\tilde{J}_{\text{NiNi}}\left(\mathbf{0}\right)\left(1-c\right)\Theta + \left(1+s_{\text{Fe}}\right)s_{\text{Fe}}\tilde{J}_{\text{FeFe}}\left(\mathbf{0}\right)c\Xi - \\ & -\Big(\Big[\left(1+s_{\text{Ni}}\right)s_{\text{Ni}}\tilde{J}_{\text{NiNi}}\left(\mathbf{0}\right)\left(1-c\right)\Theta - \left(1+s_{\text{Fe}}\right)s_{\text{Fe}}\tilde{J}_{\text{FeFe}}\left(\mathbf{0}\right)c\Xi\Big]^2 + \\ & +4\left(1+s_{\text{Ni}}\right)s_{\text{Ni}}\left(1+s_{\text{Fe}}\right)s_{\text{Fe}}\tilde{J}^2_{\text{NiFe}}\left(\mathbf{0}\right)\left(1-c\right)c\Omega^2\Big)^{1/2}\Big\}, \end{aligned} \tag{25}$$

where coefficients, Θ, Ξ, Ω, are defined as follows:

$$\Theta = 1 - \frac{1}{16}\frac{\eta_C^2}{\left(1-c\right)^2}, \ \Xi = 1 - \frac{1}{16}\frac{\eta_C^2}{c^2}, \ \Omega = 1 + \frac{1}{16}\frac{\eta_C^2}{c\left(1-c\right)}, \tag{26}$$

where $\eta_C = \eta_C(c)$ is the equilibrium atomic-LRO parameter at the Curie point, $T_C = T_C(c)$. Equation (26) is valid for a $L1_2$-type atomic-LRO state. In case of the $L1_0$-type LRO state, it is necessary to replace the factor 1/16 in (26) by 1/12.

For the atomic-SRO solid solutions, where $\eta_C \equiv 0$, Eq. (25) becomes simpler. In this case for f.c.c.-Ni–Fe alloys, it is possible to determine values of Fourier components of 'exchange' 'integrals', $\tilde{J}_{\text{NiNi}}\left(\mathbf{0}\right)$, $\tilde{J}_{\text{FeFe}}\left(\mathbf{0}\right)$, $\tilde{J}_{\text{NiFe}}\left(\mathbf{0}\right)$, at the fixed values of spin numbers, s_{Ni} and s_{Fe}, with use of experimental data on the concentration-dependent Curie temperature for these alloys. Experimental data and fitting curve obtained according to (25) are shown in Fig. 2.

Deviation of approximating curve for the $T_C(c)$ function (25) from experimental data (Fig. 2) at $c > 0.55$ is apparently conditioned by both the presence of heterogeneous (atomic and/or magnetic) states [14–24, 66] in f.c.c.-Ni–Fe alloys and the simultaneously increasing contribu-

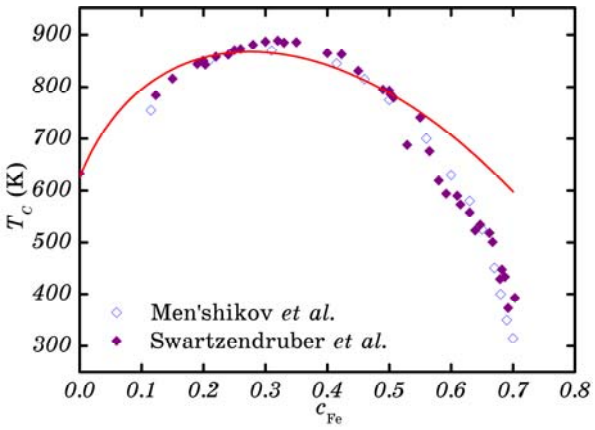

Fig. 2. Concentration dependence of Curie temperature for f.c.c.-Ni–Fe alloys, $T_C(c_{Fe})$, corresponding to the experimental data (◆, ◇) [4, 82], and the fitting curve plotted according to Eq. (25).

tion of itinerant electron magnetism into 'effective' 'exchange' interactions [75, 76]. In general case, in the measurands such as $T_C(c)$ (25), there is a combination of all parameters such as follow:

$$s_{Ni}(1+s_{Ni})\tilde{J}_{NiNi}(\mathbf{0}),\ s_{Fe}(1+s_{Fe})\tilde{J}_{FeFe}(\mathbf{0}),\ \sqrt{s_{Ni}(1+s_{Ni})s_{Fe}(1+s_{Fe})}\tilde{J}_{NiFe}(\mathbf{0}),$$

and it is difficult to determine unambiguously the values of 'exchange' 'integrals', $\{\tilde{J}_{\alpha\alpha'}(\mathbf{0})\}$ from experimental magnetic phase boundaries.

The Fourier components of 'exchange' 'integrals' estimated by the fitting of Eq. (25) to experimental data on Curie temperatures [4, 82] (Fig. 2) are shown in Table 1. (These energy parameters have been calculated for several possible combinations of values of total spin numbers, s_{Ni} and s_{Fe}, for Ni and Fe atoms, respectively.)

Considering the approximate ratio

$$\tilde{J}_{\alpha\alpha'}(\mathbf{0}) \cong 12J_{\alpha\alpha'}(r_1) \tag{27}$$

TABLE 1. Fourier components of 'exchange' 'integrals' for magnetic interactions, $\{\tilde{J}_{\alpha\alpha'}(\mathbf{k})\}$, evaluated for f.c.c.-Ni–Fe alloys.

s_{Ni}	s_{Fe}	$\tilde{J}_{NiNi}(\mathbf{0})$ (meV)	$\tilde{J}_{FeFe}(\mathbf{0})$ (meV)	$\tilde{J}_{NiFe}(\mathbf{0})$ (meV)	$\tilde{J}_{NiNi}(\mathbf{k}_X)$ (meV)	$\tilde{J}_{FeFe}(\mathbf{k}_X)$ (meV)	$\tilde{J}_{NiFe}(\mathbf{k}_X)$ (meV)
1/2	1/2	–215.9	274.6	–517.6	72.0	–91.5	172.5
1/2	1	–215.9	103.0	–316.9	72.0	–34.3	105.6
1/2	3/2	–215.9	54.9	–231.5	72.0	–18.3	77.2

TABLE 2. 'Exchange' 'integrals' for magnetic interactions within the 1st coordination shell, $J_{\alpha\alpha'}(r_{\mathrm{I}})$, for f.c.c.-$Ni_{1-c}Fe_c$ alloys.

c	s_{Ni}	s_{Fe}	$J_{\mathrm{NiNi}}(r_{\mathrm{I}})$ (meV)	$J_{\mathrm{FeFe}}(r_{\mathrm{I}})$ (meV)	$J_{\mathrm{NiFe}}(r_{\mathrm{I}})$ (meV)	References
$c \in [0, 1]$	1/2	1/2	–17.99	22.88	–43.13	Ni–Fe [present work]
$c \in [0, 1]$	1/2	1	–17.99	8.58	–26.41	
$c \in [0, 1]$	1/2	3/2	–17.99	4.58	–19.29	
$c \cong 0.75$	1/2	1/2	–22.00	5.00	–22.00	Ni–Fe[a]
$c \cong 0.50$	1/2	1/2	–22.00	5.00	–42.00	Ni–Fe[a]
$c \cong 0.25$	1/2	1/2	–22.00	5.00	–45.00	Ni–Fe[a]
$c \in [0, 1]$	0.3	3/2	–52.00	9.00	–39.00	Ni–Fe[b]
$c \cong 0.50$	0.3	3/2	–30.00	4.00	–30.00	Ni–Fe[c]
$c \cong 0.20$	0.3	3/2	–58.50	23.30	–25.5	Ni–Fe[c]
$c \in [0, 1]$	0.3	1.4	–34.90	1.70	–24.10	Ni–Fe[d]
$c \in [0, 1]$	0.3	1.4	–60.30	2.20	–30.60	Ni–Fe[e]
$c \in [0, 0.5]$	0.3	1.4	–5.30	3.30	–11.40	Ni–Fe[f]
$c \in [0, 0.5]$	0.3	1.4	–16.00	10.10	–35.00	Ni–Fe[g]

[a] [73] (cluster variation method), [b] [83] (neutron small-angle scattering technique), [c] [84] (spin-wave resonance method), [d] [79] (cluster methods in the mean-field theory), [e] [80] (Ising-type approximation in Monte Carlo simulation), [f] [78] (mean-field theory vector model and Monte Carlo simulation), [g] [77] (mean-field theory vector model and Monte Carlo simulation).

that is faithfully acceptable for short-range magnetic interactions between the 1st nearest neighbours only, it is possible to evaluate 'exchange' 'integrals' for magnetic interactions at the 1st coordination shell radius, r_{I}. As evidently from Table 2, the 'exchange' 'integrals' for magnetic interactions evaluated here within the scope of the MSCF approximation, $J_{\mathrm{NiNi}}(r_{\mathrm{I}})$ and $J_{\mathrm{NiFe}}(r_{\mathrm{I}})$, correspond to ferromagnetic interactions in the Ni–Ni and Ni–Fe pairs of spins, and $J_{\mathrm{FeFe}}(r_{\mathrm{I}})$ corresponds to the antiferromagnetic interaction in Fe–Fe pair of spins that is in a good agreement with results of other investigations of f.c.c.-Ni–Fe alloys. (A contradiction in signs of 'exchange' 'integrals' estimated here and in works of other authors is due to the opposite of $J_{\alpha\alpha'}(r_{\mathrm{I}})$ signs in their classical spin Hamiltonians; see original papers [73, 77–80, 83, 84].)

3.2. 'Direct' 'Electrochemical' Interatomic-Interaction Energies for F.C.C.-Ni–Fe Alloys

Usually, for calculations of equilibrium and kinetic characteristics of

alloys, the well-known semi-phenomenological and (or) *ab initio* methods for estimation of 'atom–atom' 'direct' 'electrochemical' interaction energies are used. 'Electrochemical' 'mixing' energy for n-th coordination shell with radius r_n, $\varphi_{chem}(r_n)$ (n = I, II, III, ...), is defined through the pair-wise interatomic-interaction energies as in Eq. (2) [25, 26, 30, 86]. Its Fourier components are defined by Eq. (5). Within the scope of the SCF approximation, it is convenient to analyze interatomic interactions within the reciprocal space (**k**-space) representation.

For the first time, the symmetry properties of interatomic 'mixing' energies have been formulated by Khachaturyan [25, 26], de Fontaine [86], Sanchez *et al.* [87], and afterwards they were generalized by Chepulskii *et al.* [59, 88] within the scope of multicomponent lattice-gas model. Below, having regard to the **k**-space symmetry properties of 'mixing' energies, we will analyze the validity of several semi-empirical and *ab initio* potentials, which were applied by other authors in various thermodynamic calculations of f.c.c.-Ni–Fe alloys, for 'electrochemical' interactions of atoms located at the geometrically perfect (unrelaxed!) f.c.c. crystal-lattice sites.

Within the Abrahamson's parameterization [89], the analytical function in the form of frequently used Born–Mayer potential consists of 'atom–atom' repulsion part only:

$$\varphi_{chem}^{\alpha\alpha'}(r_n) \approx \Psi^{\alpha\alpha'} e^{-b^{\alpha\alpha'} r_n} \quad \left(R_l^{\alpha\alpha'} \le r_n \le R_u^{\alpha\alpha'}\right). \tag{28}$$

Here, n is the number of coordination shell with radius r_n, and $R_l^{\alpha\alpha'}$, $R_u^{\alpha\alpha'}$ (α, α' = Ni, Fe) are the lower and upper limits for interatomic distance, in which the accuracy of description with this potential is high enough ($\cong$ 2–3%). For Ni–Ni atomic pairs, $\Psi^{NiNi} \approx 13271$ eV, $b^{NiNi} \approx$ ≈ 3.56819 Å^{-1}, $R_l^{NiNi} \approx 0.79376559$ Å, $R_u^{NiNi} \approx 1.85211971$ Å or $R_u^{NiNi} \approx$ $\approx 3.17506236 - 4.23341648$ Å. For Fe–Fe interactions, $\Psi^{FeFe} \approx 11931$ eV, $b^{FeFe} \approx 3.57730$ Å^{-1}, $R_l^{FeFe} \approx 0.79376559$ Å, $R_u^{FeFe} \approx 1.85211971$ Å or $R_u^{FeFe} \approx 3.17506236 - 4.23341648$ Å. For Ni–Fe pairs, $\Psi^{NiFe} \cong 12583.2$ eV, $b^{NiFe} \cong 3.57275$ Å^{-1}, $R_l^{NiFe} \cong 0.79376559$ Å, $R_u^{NiFe} \cong 1.85211971$ Å or $R_u^{NiFe} \cong 3.17506236 - 4.23341648$ Å.

In analysis of phase diagram of Ni–Fe alloys within the phase region according to atomic $L1_0$(NiFe)-type LRO, Horiuchi *et al.* have used Lennard-Jones potential in the following form [15]:

$$\varphi_{chem}^{\alpha\alpha'}(r_n) \approx \varphi_{\alpha\alpha'}^0 \left\{ \left(\frac{r_{\alpha\alpha'}}{r_n} \right)^{m_1} - \frac{m_1}{m_2} \left(\frac{r_{\alpha\alpha'}}{r_n} \right)^{m_2} \right\}. \tag{29}$$

Parameters, m_1, m_2, $\varphi_{\alpha\alpha'}^0$, $r_{\alpha\alpha'}$ (α, α' = Ni, Fe), are as follows: $m_1 \approx 7.0$, $m_2 \approx 3.5$; $\varphi_{NiNi}^0 \approx 0.7391$ eV, $r_{NiNi} \approx 2.486$ Å; $\varphi_{FeFe}^0 \approx 0.7007$ eV, $r_{FeFe} \approx$ ≈ 2.517 Å; $\varphi_{NiFe}^0 \approx 0.7919$ eV, $r_{NiFe} \approx 2.509$ Å.

Mishin *et al.* have presented in [17] the pair-wise interatomic-

interaction potentials for Ni–Fe alloys in the form of generalized Lennard-Jones potential—'angular-dependent' potential (ADP).

Dang *et al.* have considered in [81] (see also refs. therein) the interplay of magnetic order and atomic LRO in $L1_2$(Ni_3Fe)-, $L1_0$(NiFe)- and $L1_2$(Fe_3Ni)-type alloys and have offered the following adjustable values of pair-wise 'direct' 'electrochemical'-interaction energies for the 1st coordination-shell neighbours (in accordance with measured cohesive energies for pure f.c.c. α-Ni and γ-Fe): $\varphi_{\text{chem}}^{\text{NiNi}}(r_{\text{I}}) \approx -0.740$ eV, $\varphi_{\text{chem}}^{\text{FeFe}}(r_{\text{I}}) \approx$ ≈ -0.724 eV and $\varphi_{\text{chem}}^{\text{NiFe}}(r_{\text{I}}) \approx -0.793$ eV. Thus, considering Eq. (2), one can obtain the value of 'electrochemical' 'mixing' energy: $\varphi_{\text{chem}}(r_{\text{I}}) \approx$ ≈ 0.122 eV. Taylor *et al.* have chosen a similar value of 'electrochemical' 'mixing' energy [77]: $\varphi_{\text{chem}}(r_{\text{I}}) \approx 0.130$ eV.

By analogy, knowing the pair-wise 'electrochemical'-interaction energies reported in [15, 17, 81, 89] and using Eq. (2), it is possible to evaluate 'electrochemical' 'mixing' energies for each of them.

Further, using the Fourier transform defined by Eq. (5), we have obtained the dispersion dependences for Fourier components of 'electrochemical' 'mixing' energies for h-s points and the main symmetry directions within the irreducible region of the 1st *BZ* for f.c.c. lattice; see Fig. 3. Here, the recalculated energies for the Invar-like $Fe_{0.65}Ni_{0.35}$ alloy originally computed by Ruban *et al.* within the scope of the exact muffin-tin orbital–coherent potential approximation–generalized perturbation method (EMTO–CPA–GPM) for paramagnetic state (DLM) and ferromagnetic (FM) one (see Fig. 1 in [90]) and the many-body interatomic po-

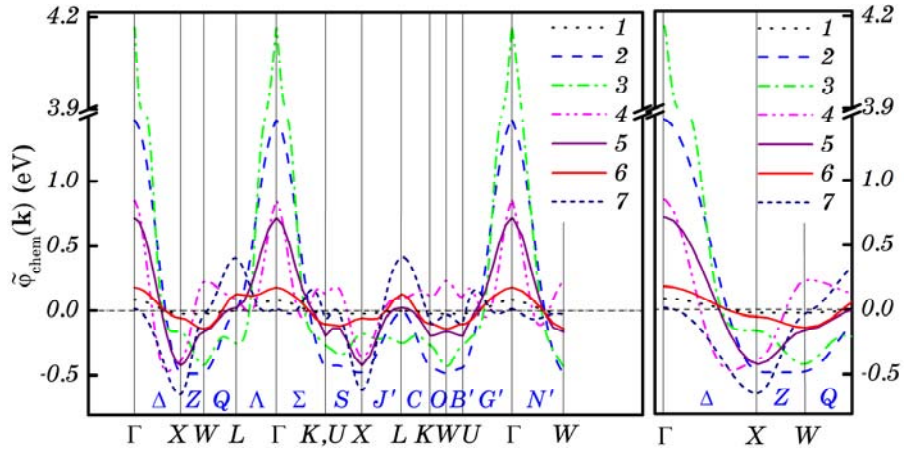

Fig. 3. Dispersion curves for Fourier components of 'electrochemical' 'mixing' energies, $\tilde{\varphi}_{\text{chem}}(\mathbf{k})$, along the main directions between the h-s points within the irreducible region of the 1st *BZ* for f.c.c.-Ni–Fe alloys, which were calculated according to pair-wise energies (in direct **r**-space) reported in [89, 81, 15, 17, 90, 91] (see curves *1*, *2*, *3*, *4*,(*5*, *6*) and *7*, respectively).

tential based on the embedded atom method (EAM) formalism and reported by Bonny *et al.* [91] are also presented.

As evident in Figure 3, Fourier components of 'electrochemical' 'mixing' energies estimated with a potential parameterization reported in [89] do not contradict the symmetry requirements, but energy magnitudes are underestimated, and a global minimum of the 'mixing'-energy Fourier components ($\tilde{\varphi}_{\text{chem}}(\mathbf{k}_X) = \tilde{\varphi}_{\text{chem}}(\mathbf{k}_W)$) is simultaneously at the $W(1\ \frac{1}{2}\ 0)$ and $X(0\ 0\ 1)$ points that follows from Eq. (5) with restriction on interaction potential by the 1st coordination shell and corresponds to the occurrence of $D0_{22}$-type layered f.c.t. structure, which is not observed in Ni–Fe alloys.

The same conclusion concerns the energies reported in [81]. Nevertheless, their values have been used by authors of this paper in the Monte Carlo simulations of atomic-ordering phenomena in Ni–Fe alloys, although they have not monitored the local atomic distributions within the modelled crystallites in direct space that would reveal serious shortcomings of chosen 'electrochemical'-interaction potential extended to the first nearest neighbours only.

As regards energies evaluated in [15], obviously, a minimum of the 'mixing'-energy Fourier components is located at the $W(1\ \frac{1}{2}\ 0)$ point only that corresponds to appearance of hypothetical A_2B_2-type [25, 26] layered (super)structure, which is also not observed in f.c.c.-Ni–Fe alloys.

Dispersion dependence of 'electrochemical' 'mixing'-energy Fourier components calculated according to 'angular-dependent' potential reported in [17] manifests itself as the best of all considered above. The value of such Fourier component at the h-s $X(0\ 0\ 1)$ point is sufficient to reproduce the realistic order–disorder phase-transformation temperature (for instance, close to its values given for $L1_2$-Ni_3Fe-type structures by means of Monte Carlo simulation only). The circumstance that a global minimum of the 'mixing'-energy Fourier components is not at the $X(0\ 0\ 1)$ point but in its vicinity testifies to the occurrence of (super)structure, which differs from known $L1_2$- and $L1_0$-type structures, or the appearance of long-period structures based on the stacking-faulted $L1_2$- or $L1_0$-type structures, which are also not observed in f.c.c.-Ni–Fe alloys.

Concerning energies calculated on the basis of data reported in [90], it is evident (see curves *5*, *6* in Fig. 3) that a minimum of the 'mixing' energy Fourier components for f.c.c.-Ni–Fe alloys in the DLM state is observed at the $W(1\ \frac{1}{2}\ 0)$ point just like the case of 'electrochemical' energies obtained in [15].

Besides, for the FM state of alloys at issue, the minimum is located at the $X(0\ 0\ 1)$ point, though its overestimated magnitude is so high that it gives the alloy instability temperature, which appears much higher than experimental one.

Fourier components of 'mixing' energies obtained with data [91]

have an excessively deep (overestimated) minimum at the $X(0\,0\,1)$ point, nevertheless, their value at the 'fundamental' $\Gamma(0\,0\,0)$ points is near-zero that testifies to the possibility of f.c.c. disordered phase in a metastable state.

Thus, none of the mentioned potentials of 'electrochemical' interaction can be applied adequately in the statistical-thermodynamic analysis of f.c.c.-Ni–Fe alloys, and in some cases, they contradict the symmetry properties of observed phases (in paramagnetic or ferromagnetic states with $L1_2$-type and (or) $L1_0$-type atomic LRO) and respective 'mixing' energy Fourier transforms (see [25, 26, 85–88] for details). At the same time, all the specified 'mixing' potentials can be successfully used for a fitting of other 'macroscopically-average' characteristics of an alloy (such as its elastic modules, equilibrium lattice spacing parameter, cohesive energy, *etc*.) defined by the 'mixing' potentials and (or) their spatial derivatives.

3.3. 'Strain-Induced' Interatomic-Interaction Energies of Dissolved Atoms in Solid Solutions Based on the F.C.C. Host Metal: the Salient Features of α-Ni–Fe and γ-Fe–Ni Solutions

It is well known [25, 26, 36, 37, 92–104] that the interatomic interactions in real alloys are much more complex and not limited only by the short-range 'direct' 'electrochemical' interactions. One of the essential contributions to the alloy energy is the so-called 'strain-induced' interaction of dissolved (substitutional and/or interstitial) atoms. Such an interaction is anisotropic, long-range and 'quasi-oscillating' in its dependence on interatomic distance and arises because of interference of the local static distortions of a host-crystal lattice due to introduction of alloying atoms.

For the first time, the consistent microscopic theory of 'strain-induced' interaction was formulated in the works of Khachaturyan [92, 93], Cook and de Fontaine [94, 95] based on representation of interaction characteristics in reciprocal space by means of the Matsubara–Kanzaki–Krivoglaz lattice-statics method [96]. Following this theory [25, 26, 92–104], the 'strain-induced' interaction energies, $V_{\text{si}}^{\alpha\alpha}\left(\mathbf{R}-\mathbf{R}'\right)$, of α–α pairs of dissolved atoms within the primitive unit cells distant from each other at some spacing $\mathbf{r}=\mathbf{R}-\mathbf{R}'$, can be expanded into finite Fourier series as follows:

$$V_{\text{si}}^{\alpha\alpha}\left(\mathbf{R}-\mathbf{R}'\right)=N_{\text{u.c.}}^{-1}\sum_{\mathbf{k}\in 1^{\text{st}}BZ}\tilde{V}_{\text{si}}^{\alpha\alpha}\left(\mathbf{k}\right)e^{+i\mathbf{k}\cdot\mathbf{r}}\ . \tag{30}$$

Here, summation is made over all $N_{\text{u.c.}}$ points of quasi-continuum $\{\mathbf{k}\}$ within the 1^{st} *BZ* for f.c.c. lattice; $\tilde{V}_{\text{si}}^{\alpha\alpha}\left(\mathbf{k}\right)$ is the $\mathbf{k}$-th Fourier component of 'strain-induced' interaction energies.

According to [26], $\tilde{V}_{\text{si}}^{\alpha\alpha}(\mathbf{k})$ can be expressed in terms of the concentration coefficients of dilatation of a host-crystal lattice, $L^{\alpha} = \{\partial \ln a / \partial c_{\alpha}\}\big|_{c_{\alpha}=0}$, modules of elasticity, C_{IJ}, and/or one longitudinal frequency and two transversal frequencies of natural quasi-harmonic vibrations of a host crystal, $\omega_{\text{L}}(\mathbf{k})$, $\omega_{\text{T1}}(\mathbf{k})$, $\omega_{\text{T2}}(\mathbf{k})$.

Within the scope of the superposition [26] and quasi-harmonic [97] approximations, the Fourier components of 'strain-induced' interaction energies are defined as follows:

$$\tilde{V}_{\text{si}}^{\alpha\alpha}(\mathbf{k}) \approx -\sum_{i,j=x,y,z} \tilde{F}^{i*}(\mathbf{k}) \tilde{G}^{ij}(\mathbf{k}) \tilde{F}^{j}(\mathbf{k}) + N_{\text{u.c.}}^{-1} \sum_{\mathbf{k}'\neq\mathbf{0}} \sum_{i,j=x,y,z} \tilde{F}^{i*}(\mathbf{k}') \tilde{G}^{ij}(\mathbf{k}') \tilde{F}^{j}(\mathbf{k}') \quad \text{for } \mathbf{k} \neq \mathbf{0}, \tag{31}$$

$$\tilde{V}_{\text{si}}^{\alpha\alpha}(\mathbf{0}) \approx -3\upsilon (C_{11} + 2C_{12}) L^{\alpha 2} + N_{\text{u.c.}}^{-1} \sum_{\mathbf{k}'\neq\mathbf{0}} \sum_{i,j=x,y,z} \tilde{F}^{i*}(\mathbf{k}') \tilde{G}^{ij}(\mathbf{k}') \tilde{F}^{j}(\mathbf{k}'). \tag{32}$$

$\tilde{V}_{\text{si}}^{\alpha\alpha}(\mathbf{k})$ is defined in Eqs. (31), (32) for all $\mathbf{k} \in 1^{\text{st}}$ *BZ*, but it is a non-analytical function at $\mathbf{k} = \mathbf{0}$. Here, $\tilde{\mathbf{F}}(\mathbf{k})$ is the Fourier transform of 'coupling' forces (so-called Kanzaki forces) [26, 97]; $\tilde{\mathbf{G}}(\mathbf{k}) = [\tilde{\mathbf{A}}(\mathbf{k})]^{-1}$ ($\mathbf{k} \neq \mathbf{0}$); $\mathbf{A}(\mathbf{k})$ is the Fourier transform of dynamic matrix of a host crystal [26, 97]; $i, j = x, y, z$ are the Cartesian indices; $\upsilon = a_0^3/4$ is the volume of a primitive unit cell; C_{11} and C_{12} are the elastic modules.

When Kanzaki forces, $\mathbf{F}(\mathbf{R} - \mathbf{R}')$, are nonzero for the 1^{st} nearest-neighbour coordination shell of sites around the dissolved substitutional atom and are directed along a straight line from the impurity atom towards the host-crystal atom, $\tilde{\mathbf{F}}(\mathbf{k})$ has a following form [97]:

$$\tilde{\mathbf{F}}(\mathbf{k}) \cong -i \frac{a_0^2}{4} (C_{11} + 2C_{12}) L^{\alpha} \left\| \begin{array}{l} \sin\left(\frac{a_0}{2} k_x\right) \left[\cos\left(\frac{a_0}{2} k_y\right) + \cos\left(\frac{a_0}{2} k_z\right)\right] \\ \sin\left(\frac{a_0}{2} k_y\right) \left[\cos\left(\frac{a_0}{2} k_z\right) + \cos\left(\frac{a_0}{2} k_x\right)\right] \\ \sin\left(\frac{a_0}{2} k_z\right) \left[\cos\left(\frac{a_0}{2} k_x\right) + \cos\left(\frac{a_0}{2} k_y\right)\right] \end{array} \right\|. \tag{33}$$

The 'strain-induced' interaction energies calculated in [98, 99, 102] for f.c.c. γ-Fe- and α-Ni-based solid solutions are listed in Table 3.

According to [1, 105], dependence of a lattice parameter for α-Ni [105] (or γ-Fe [1]) on concentration of dissolved Fe (Ni) atoms, $a_{\text{Ni}}(c_{\text{Fe}})$ ($a_{\text{Fe}}(c_{\text{Ni}})$), changes under the well-known Végard's 'law': $a_{\text{Ni}}(c_{\text{Fe}}) \approx a_{\text{Ni}}^0 + [da_{\text{Ni}}/dc_{\text{Fe}}]_0 c_{\text{Fe}} = a_{\text{Ni}}^0[1 + L^{\text{Fe}} c_{\text{Fe}}]$, $a_{\text{Fe}}(c_{\text{Ni}}) \approx a_{\text{Fe}}^0 + [da_{\text{Fe}}/dc_{\text{Ni}}]_0 c_{\text{Ni}} = a_{\text{Fe}}^0[1 + L^{\text{Ni}} c_{\text{Ni}}]$, and at some concentration, c_{Ni}, the value of L^{Ni} changes a sign (see Table 4 and [1]).

TABLE 3. The 'strain-induced' interaction energies between the substitutional dissolved atoms, $V_{si}^{\alpha\alpha}(\mathbf{R}-\mathbf{R}')$ (α = Fe, Ni), in f.c.c. host crystal (α-Ni [98, 99] and γ-Fe [98, 102], respectively).

$2(\mathbf{R}-\mathbf{R}')/a_0$	110	200	211	220	310	222	321	400	330	411
No. shells	I	II	III	IV	V	VI	VII	VIII	IX_l	IX_u
$\lvert\mathbf{R}-\mathbf{R}'\rvert/a_0$	≈ 0.71	1	≈ 1.22	≈ 1.41	≈ 1.58	≈ 1.73	≈ 1.87	2	≈ 2.12	≈ 2.12
$V_{si}^{FeFe}(\mathbf{R}-\mathbf{R}')$ (meV)[a]	−4.8	−1.3	+0.3	+0.7	−0.3	+0.06	+0.08	−0.2	+0.2	−0.1
$V_{si}^{FeFe}(\mathbf{R}-\mathbf{R}')$ (meV)[b]	−5.3	−1.5	+0.3	+0.7	−0.4	+0.08	+0.08	−0.2	+0.2	−0.2
$V_{si}^{NiNi}(\mathbf{R}-\mathbf{R}')$ (meV)[a]	−0.2	−0.07	+0.009	+0.03	−0.02	+0.01	+0.004	−0.009	+0.009	−0.009
$V_{si}^{NiNi}(\mathbf{R}-\mathbf{R}')$ (meV)[c]	$-4\cdot10^{-3}$	$-1\cdot10^{-3}$	$+2\cdot10^{-4}$	$+5\cdot10^{-4}$	$-4\cdot10^{-4}$	$+2\cdot10^{-4}$	$+8\cdot10^{-5}$	$-2\cdot10^{-4}$	$+2\cdot10^{-4}$	$-2\cdot10^{-4}$

[a][98], [b][99], [c][102].

TABLE 4. Experimental data used in a given work for calculation of 'strain-induced' interaction parameters for f.c.c. γ-Fe- or α-Ni-based solid solutions.

Host crystal	Concentrations of dissolved atoms, c_α	C_{11}, C_{12}, C_{44} (GPa)	$\omega_L(\mathbf{k}_X)$ (Trad·s^{-1})	$\omega_T(\mathbf{k}_X)$ (Trad·s^{-1})	L^{Ni}	L^{Fe}
γ-Fe	$c_{Ni} \in [0, 0.29]$	154, 122, 77[c]	46.88[c]	33.85[c]	$L_1^{Ni} \approx -0.007$[a]	—
	$c_{Ni} \in [0.29, 0.4]$				$L_2^{Ni} \approx +0.001$[a]	—
α-Ni	$c_{Fe} \in [0, 0.6]$	240, 149, 116[d]	53.72[d]	39.40[d]	—	+0.033[b]

[a][1], [b][105], [c][106], [d][107]. Data are given for f.c.c. γ-Fe at 1428 K and α-Ni at 300 K.

Difference between the 'strain-induced' energies, $V_{si}^{NiNi}(\mathbf{R} - \mathbf{R}')$, obtained in [98, 102] (see Table 3) is due to the distinction in used values of concentration coefficient, L^{Ni}, for considered γ-Fe–Ni solutions.

Using the data from Table 4 and, for simplicity only, assuming independence of 'strain-induced' interaction energies on temperature, the dispersion dependences of Fourier components, $\tilde{V}_{si}^{\alpha\alpha}(\mathbf{k})$, for α atoms in γ-Fe or α-Ni (Fig. 4), and their 'concentration' dependences (Fig. 5) were calculated.

There are some relationships, which are significant for the priority rating of governing factors in the statistical thermodynamics of substitutional solid solutions based on f.c.c. lattice. Namely, for the h-s

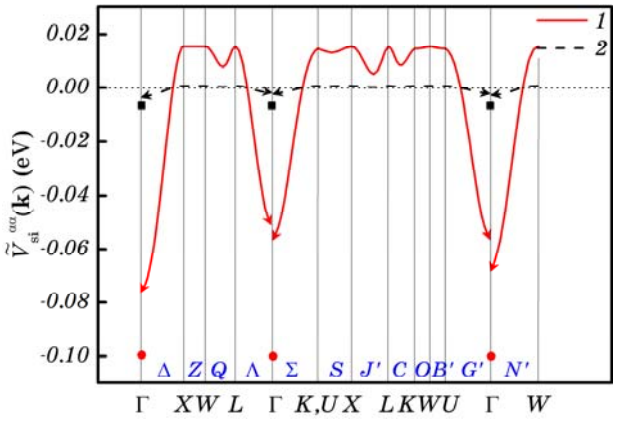

Fig. 4. Dispersion dependences of 'strain-induced' interaction energy Fourier components for dissolved atoms, $\tilde{V}_{si}^{\alpha\alpha}(\mathbf{k})$ (αα = NiNi, FeFe), in f.c.c. γ-Fe and α-Ni along the main directions between the h-s points within the irreducible region of the 1st *BZ*; *1*, *2*— $\tilde{V}_{si}^{FeFe}(\mathbf{k})$ and $\tilde{V}_{si}^{NiNi}(\mathbf{k})$ dependences, respectively, estimated for any $\mathbf{k} \in$ 1st *BZ* including $\mathbf{k} \to \mathbf{0}$ (31) and $\mathbf{k} = \mathbf{k}_\Gamma = \mathbf{0}$ (32); ●— $\tilde{V}_{si}^{FeFe}(\mathbf{0})$, ■— $\tilde{V}_{si}^{NiNi}(\mathbf{0})$. Here, $L^{Ni} \approx -0.007$ and $L^{Fe} \approx +0.033$ (see Table 4). Calculations are carried out for solid solutions based on f.c.c. γ-Fe (at 1428 K) and α-Ni (at 300 K) (see also Table 4).

points, $\{\Gamma, X, W, L, K(U)\}$, in the 1st *BZ*:

$$\tilde{V}_{\mathrm{si}}^{\alpha\alpha}(\mathbf{0}) < \tilde{V}_{\mathrm{si}}^{\alpha\alpha}(\mathbf{k}\to\mathbf{0}) < 0 < \tilde{V}_{\mathrm{si}}^{\alpha\alpha}(\mathbf{k}_X) = \tilde{V}_{\mathrm{si}}^{\alpha\alpha}(\mathbf{k}_W) = \tilde{V}_{\mathrm{si}}^{\alpha\alpha}\left(\mathbf{k}_{K(U)}\right) = \tilde{V}_{\mathrm{si}}^{\alpha\alpha}(\mathbf{k}_L) \quad (34)$$

(as a rule, within the scope of the approximation [97] according to Eq. (33) and if $C_{12} < C_{11}$); see Fig. 4.

Thus, according to Table 3 and Figure 4, it is evident that 'strain-induced' interaction energies are long-range, anisotropic (*e.g.*, over IX-th coordination shells), and not equal to zero even for the distant coordination shells. Fourier components of these energies, $\tilde{V}_{\mathrm{si}}^{\alpha\alpha}(\mathbf{k})$, along various directions from the surface h-s points to the Γ(0 0 0) point behave in different ways (and discontinuities of the first kind of the $\tilde{V}_{\mathrm{si}}^{\alpha\alpha}(\mathbf{k})$ function take place at $\mathbf{k}_\Gamma = \mathbf{0}$): $\tilde{V}_{\mathrm{si}}^{\alpha\alpha}(\mathbf{0}) < \tilde{V}_{\mathrm{si}}^{\alpha\alpha}\left(\mathbf{k}\xrightarrow[\mathbf{k}\downarrow\uparrow\mathbf{k}_X]{}\mathbf{0}\right) <$ $< \tilde{V}_{\mathrm{si}}^{\alpha\alpha}\left(\mathbf{k}\xrightarrow[\mathbf{k}\downarrow\uparrow\mathbf{k}_W]{}\mathbf{0}\right) < \tilde{V}_{\mathrm{si}}^{\alpha\alpha}\left(\mathbf{k}\xrightarrow[\mathbf{k}\downarrow\uparrow\mathbf{k}_{K(U)}]{}\mathbf{0}\right) < \tilde{V}_{\mathrm{si}}^{\alpha\alpha}\left(\mathbf{k}\xrightarrow[\mathbf{k}\downarrow\uparrow\mathbf{k}_L]{}\mathbf{0}\right)$ (as far as $C_{11} - C_{12} - 2C_{44} < 0$ and $C_{12} < C_{11}$) that confirms non-analytical behaviour, long-range character and anisotropy of 'elastic' interaction between dissolved impurity atoms in f.c.c.-Ni–Fe alloys.

Besides, as follows from Figures 4 and 5, there is a significant difference between the interaction energies for solid solutions based on γ-Fe and α-Ni that corresponds to the different interaction energies for f.c.c.-Ni–Fe alloys at compositions close to Invar ($L1_2$-Fe_3Ni) and

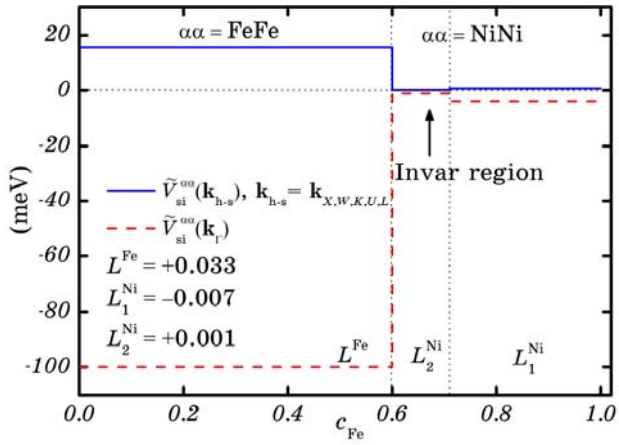

Fig. 5. 'Concentration' dependences of Fourier components of 'strain-induced' interaction energies, $\tilde{V}_{\mathrm{si}}^{\alpha\alpha}(\mathbf{k}_{\Gamma,\mathrm{h\text{-}s}}, c_{\mathrm{Fe}})$, for dissolved α atoms in f.c.c. γ-Fe or α-Ni calculated for 'fundamental' Γ(0 0 0) point and superstructural h-s points, $\{X, W, L, K(U)\}$, in the 1st *BZ*. Calculations are carried out for f.c.c. γ-Fe or α-Ni at $T = 1428$ and $T = 300$ K, respectively (see also Table 4).

Permalloy ($L1_2$-Ni_3Fe). Jumps of Fourier components, $\tilde{V}_{si}^{\alpha\alpha}\left(\mathbf{k}_{\Gamma,h\text{-}s}, c_\alpha\right)$, at $c_{Fe} = 0.6$ and $c_{Ni} = 0.29$ (see Fig. 5) are conditioned by the changes in L^{Ni} value at these concentrations and probably correspond to transition of electron subsystem of Fe atoms from one electronic state to another or to transition to the state of coexistence of two and more equilibrium electronic states that, by-turn, testifies to the probable presence of two γ-states [18–24, 66] of Fe atoms in appropriate composition region.

To calculate the temperature dependences of 'strain-induced' energy Fourier components, $\tilde{V}_{si}^{FeFe}\left(\mathbf{k}_{\Gamma,h\text{-}s}, T\right)$, at the h-s points, {Γ, X, W, L, $K(U)$}, for dissolved Fe atoms in f.c.c. α-Ni, we use approximate semi-phenomenological expressions for quasi-harmonic frequencies of longitudinal and transversal vibrations of a host crystal by means of its lattice parameter and elastic modulus [85]:

$$\omega_L(T) \cong \sqrt{\frac{8a_0(T)C_{44}(T)}{M}}\,,\ \omega_T(T) \cong \frac{\omega_L(T)}{\sqrt{2}}\,. \qquad (35)$$

Here, $M = 9.748 \cdot 10^{-26}$ kg is the Ni-atom mass; $C_{44}(T)$, $a_0(T)$ are the temperature-dependent elastic modulus and lattice parameter of pure f.c.c. Ni, respectively. In presentation of the $C_{IJ}(T)$ and $a_0(T)$ dependences as $C_{IJ}(T) \cong C_{IJ}(0) + [dC_{IJ}/dT]|_{T=0K} T$ and $a_0(T) \cong a_0(0) + [da_0/dT]|_{T=0K} T$, according to [105], $C_{11}(0) \cong 264.73$ GPa, $C_{12}(0) \cong 151.23$ GPa, $C_{44}(0) \cong 133.58$ GPa, $[dC_{11}/dT]|_{T=0K} \cong -0.0526$ GPa·K^{-1}, $[dC_{12}/dT]|_{T=0K} \cong -0.0052$ GPa·K^{-1}, $[dC_{44}/dT]|_{T=0K} \cong -0.0358$ GPa·K^{-1}, $a_0(0) \cong 3.4982(7)$ Å, $[da_0/dT]|_{T=0K} \cong$ $\cong 6.0 \cdot 10^{-5}$ Å·K^{-1}. Substituting temperature-dependent $C_{44}(T)$ and $a_0(T)$ into Eq. (35) and using the approximations $\omega_L \cong \omega_L(0) + [d\omega_L/dT]|_{T=0K} T$, $\omega_T \cong \omega_T(0) + [d\omega_T/dT]|_{T=0K} T$, we have the following estimations: $\omega_L(0) \cong$ $\cong 61.992$ Trad·s^{-1}, $\omega_T(0) \cong 43.835$ Trad·s^{-1}, $[d\omega_L/dT]|_{T=0K} \cong -0.0083$ Trad·s^{-1}·K^{-1}, $[d\omega_T/dT]|_{T=0K} \cong -0.0059$ Trad·s^{-1}·K^{-1}.

Using the calculated data for Fe atoms dissolved in f.c.c. α-Ni, it is possible to plot 'strain-induced' interaction energy Fourier components, $\tilde{V}_{si}^{FeFe}\left(\mathbf{k}_{\Gamma,h\text{-}s}, T\right)$, versus the temperature (Fig. 6). (Such parameters, $\tilde{V}_{si}^{NiNi}\left(\mathbf{k}, T\right)$, for Ni atoms dissolved in f.c.c. γ-Fe have not evaluated because of lack of the reliable data on temperature dependence of $C_{IJ}(T)$, $\omega_L(T)$, and $\omega_T(T)$ for γ-Fe.) As shown in Fig. 6, the evaluated parameters, $\tilde{V}_{si}^{FeFe}\left(\mathbf{k}_{\Gamma,h\text{-}s}, T\right)$, linearly depend on T, and within the temperature range of 0–1000 K, the magnitudes of their relative change are equal to $\cong 10\%$. Such a change of 'strain-induced' interaction energies is not significant. As it will be shown below, it is possible to neglect their temperature dependence in comparison with the temperature dependence of magnetic contribution, $\tilde{w}_{mag}\left(\mathbf{k}, T\right)$, into the 'mixing' energy of an alloy.

3.4. Total Interatomic 'Mixing' Energies for F.C.C.-Ni–Fe Alloys

We have consecutive considered all main types of the interatomic in-

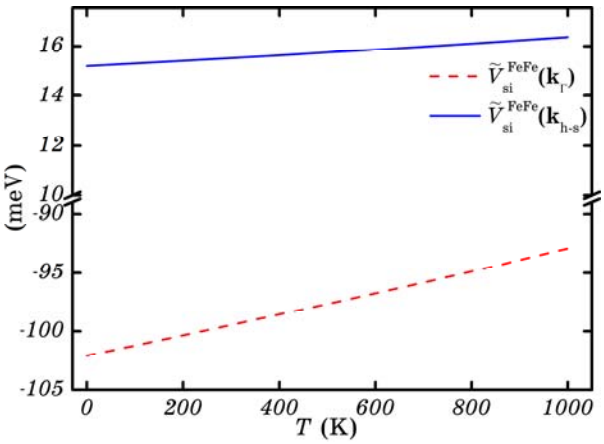

Fig. 6. Temperature-dependent 'strain-induced' interaction energy Fourier components for Fe atoms dissolved in f.c.c. α-Ni, $\tilde{V}_{si}^{FeFe}(\mathbf{k},T)$, evaluated for the h-s points, {Γ, X, W, L, $K(U)$}, in the 1st BZ.

teractions arising in (para)magnetic substitutional f.c.c.-Ni–Fe solid solutions. The sum of all energy contributions gives total 'mixing' energies of an alloy, but only some of these contributions dominate other ones in all equilibrium parameters of an alloy (including critical ones). The technique of elastic diffuse scattering of X-rays (or thermal neutrons) by SRO fluctuations of concentration in solid solutions with atomic SRO only is the unique experimental method, which may be useful to extract the information on total 'mixing' energies, correlation parameters, *etc*. in alloys. Within the scope of the SCF approximation, in case of the equilibrium alloy considerably above the order–disorder phase transformation temperature (Kurnakov's point, T_K), the expression for **k**-space distributed intensities of radiation diffuse scattering is given by the conventional Krivoglaz–Clapp–Moss (KCM) formula [25, 26, 30, 39–42]:

$$I_{\text{SRO}}(\mathbf{k}) = |f_B - f_A|^2 \langle |\tilde{C}(\mathbf{k})|^2 \rangle e^{-2\mathcal{M}-\mathcal{L}} \approx N_{\text{u.c.}} |f_B - f_A|^2 \tilde{\varepsilon}(\mathbf{k}) e^{-2\mathcal{M}-\mathcal{L}} \equiv$$

$$\equiv N_{\text{u.c.}} |f_B - f_A|^2 c(1-c)\tilde{\alpha}(\mathbf{k}) e^{-2\mathcal{M}-\mathcal{L}} \cong N_{\text{u.c.}} |f_B - f_A|^2 \frac{\mathcal{D}c(1-c)e^{-2\mathcal{M}-\mathcal{L}}}{1 + c(1-c)\dfrac{\tilde{w}_{\text{tot}}(\mathbf{k})}{k_B T}}. \quad (36)$$

Here, $f_A(\mathbf{k})$, $f_B(\mathbf{k})$ are the atomic (or nuclear, $b_A(\mathbf{k})$, $b_B(\mathbf{k})$) scattering factors. $N_{\text{u.c.}}$ is the number of primitive unit cells; c is the relative fraction of alloying B atoms; exp[–(2$\mathcal{M}$ + $\mathcal{L}$)] is the Debye–Waller factor describing a full attenuation of the interferential maxima due to the thermal (exp[–2$\mathcal{M}$]) and local static (exp[–$\mathcal{L}$]) displacements of atoms from

Bravais lattice sites; $N_{\text{u.c.}}|f_B(\mathbf{k}) - f_A(\mathbf{k})|^2 c(1-c)$ is the so-called Laue factor, which determines dependence of diffuse scattering background from the module of a scattering quasi-wave vector, $|\mathbf{k}|$, in the absence of crystal-lattice imperfections of a solid solution (SRO, linear and square static and dynamic local distortions, *etc.*); $\tilde{\varepsilon}(\mathbf{k})$ and $\tilde{\alpha}(\mathbf{k})$ are the Fourier components of correlation and Warren–Cowley SRO parameters, respectively, for A–B solid solution; $\tilde{w}_{\text{tot}}(\mathbf{k})$ (15) is the Fourier component of total 'mixing' energies of an alloy. Fourier component of site occupation numbers fluctuations, $\tilde{C}(\mathbf{k})$, is defined by the summation made over all $N_{\text{u.c.}}$ sites of the Bravais lattice, $\{\mathbf{R}\}$, as follows:

$$\tilde{C}(\mathbf{k}) = \sum_{\mathbf{R}} (C_{\mathbf{R}} - c)\, e^{-i\mathbf{k}\cdot\mathbf{R}} \,. \tag{37}$$

In Equation (36), $\langle ... \rangle$ means a statistical-ensemble averaging procedure. The value of $\tilde{\alpha}(\mathbf{k})$ is defined as:

$$\tilde{\alpha}(\mathbf{k}) = \sum_{\mathbf{r}} \alpha(\mathbf{r})\, e^{-i\mathbf{k}\cdot\mathbf{r}} \,, \tag{38}$$

where $\alpha(\mathbf{r})$ is the Warren–Cowley SRO parameter defined by the deviation of probability of finding of A (B)-kind atom at a distance $\mathbf{r}$ from B (A)-kind atom, $P^{AB}(\mathbf{r}) = \{c_B - \langle C_{\mathbf{r}} C_0 \rangle\}/c_B$ ($P^{BA}(\mathbf{r}) = \{c_B - \langle C_{\mathbf{r}} C_0 \rangle\}/c_A$), from the average concentration of A (B) atoms, $c_A = 1 - c$ ($c_B = c$), in an alloy at issue:

$$\alpha(\mathbf{r}) = 1 - \frac{P^{AB}(\mathbf{r})}{c_A} \text{ or } \alpha(\mathbf{r}) = 1 - \frac{P^{BA}(\mathbf{r})}{c_B} \text{ for } \mathbf{r} \neq \mathbf{0};\ \alpha(\mathbf{0}) = 1 \,. \tag{39}$$

Providing the last Eq. (39), normalization factor in Eq. (36) $\mathcal{D}(T, c)$, is equal to 1 accurate within 3% .

Let us consider the results of works [108–119] on diffuse scattering of radiations to study the SRO structure in f.c.c.-Ni–Fe alloys of various compositions at different temperatures. Lefebvre *et al.* [108, 109] and Bley *et al.* [110] have used a technique of elastic thermal-neutron diffuse scattering from the SRO in $^{62}Ni_{0.765}Fe_{0.235}$ solid solution to investigate the time-dependent evolution [110] of diffuse-scattering intensity distribution in $\mathbf{k}$-space at different isothermal-annealing temperatures, T_a, during the diffusion-controlled SRO relaxation to equilibrium states and its equilibrium pattern [108, 109]. Microscopic activation characteristics of the SRO relaxation kinetics were determined [110].

Ice *et al.* [111, 114–117], Jiang *et al.* [112, 113], Robertson *et al.* [118] have managed to apply a unique technique of anomalous X-ray scattering to study the local atomic configurations and the local individual-pair atomic displacements in $Ni_{0.775}Fe_{0.225}$ Permalloy [111, 113–117], $Ni_{0.535}Fe_{0.465}$ Elinvar [112–117], $Fe_{0.632}Ni_{0.368}$ Invar [118]. By means of thermal-neutron diffuse scattering, Cenedese *et al.* [119]

have investigated the same structure features (and 'mixing' energies) of $Fe_{0.698}{}^{62}Ni_{0.302}$ Invar.

As a result of investigation of the salient features of crystal-lattice local-distortion fields in the Invar-type alloy, additional opportunities are given to us to understand deeply the nature of Invar state.

Following the cited works, we have selected the radiation diffuse-scattering intensities, $I_{\mathrm{SRO}}(\mathbf{k})$, for some h-s quasi-wave vectors in reciprocal space for f.c.c.-lattice-based alloys under investigation, and, within the scope of the SCF approximation with use of the KCM formula (36), the appropriate Fourier components of total 'mixing' energies have been evaluated (see Table 5).

Diffuse scattering intensity at the 'fundamental' point, $I_{\mathrm{SRO}}(\mathbf{k}_\Gamma)$, has been extracted by its extrapolation to Γ(0 0 0) point [108–110, 119] from points lying at the distance of 0.1 units of reciprocal-lattice parameter from 'fundamental' reflection.

In works reported in [111–118], diffuse scattering intensity at the 'fundamental' point, $I_{\mathrm{SRO}}(\mathbf{0})$, has been obtained by extrapolation and by means of recalculation of Warren–Cowley SRO parameters.

One can see from Table 5, Fourier components of total 'mixing' energies are substantially concentration- and temperature-dependent quantities. As it will be shown, these dependences are mostly due to the temperature and concentration dependences of some contributions to total 'mixing' energies and are complicated probably by the appearance of local magnetic and atomic inhomogeneities within the alloy, especially, close to Invar concentration region as critical-point effects.

Using the symmetry properties [25, 26, 86–88] of both the total 'mixing' energies in direct space and their Fourier components within the 1^{st} *BZ*, $\tilde{w}_{\mathrm{tot}}(\mathbf{k})$ (Table 5), we have calculated total 'mixing' energies for quite a few coordination shells, $w_{\mathrm{tot}}(\mathbf{R}-\mathbf{R}')$, too. These results together with similar energy data by other authors are listed in Table 6. It is important to note that all estimations of total 'mixing' energies for f.c.c.-Ni–Fe alloys extracted from diffraction data obtained by other authors and listed in a given article can be changed and/or corrected likewise in view of the fact that the diffuse-scattering intensity pattern of common occurrence in practice is not equilibrium (!). For determination of equilibrium diffuse-scattering pattern and appropriate interaction energies, it is necessary to perform the experiments on time evolution of diffuse scattering intensities and thereupon to estimate theoretically the equilibrium SRO intensities, $I_{\mathrm{SRO}}(\mathbf{k}, t\to\infty)$ (see fundamental papers of Khachaturyan [121], Cook *et al.* [122], Krivoglaz *et al.* [123], Semenovskaya *et al.* [124], Bley *et al.* [110], and publications of authors of a given article [125, 126]).

Just so, it is possible to evaluate both the microscopic characteristics of migration of each constituent (for atomic-scale diffusion acts inherently) and the equilibrium thermodynamic parameters of alloys.

TABLE 5. Diffuse-scattering intensities, $I_{\mathrm{SRO}}(\mathbf{k}, T_a)$, obtained from single-crystalline samples of f.c.c.-Ni–Fe alloys with various compositions in equilibrium states after heat treatments. Fourier components of total 'mixing' energies, $\tilde{w}_{\mathrm{tot}}(\mathbf{k}, T_a)$, have been estimated according to Eq. (36).

Components of quasi-wave vector			T_a (K)		Alloys, measuring techniques
			$I_{\mathrm{SRO}}(\mathbf{k}, T_a)$	$\tilde{w}_{\mathrm{tot}}(\mathbf{k}, T_a)$	
q_x	q_y	q_z	(Laue units/atom)	(eV)	
			801		
0	0	1	6.06	–0.325	
0	0	0	0.252	+1.140	
			783		
0	0	1	9.5	–0.334	
0	0	0	0.250	+1.129	
			776		$^{62}Ni_{0.765}Fe_{0.235}$, thermal neutron scattering[a]
0	0	1	10.88	–0.338	
0	0	0	0.249	+1.124	
			773		
0	0	1	12.73	–0.341	
0	0	0	0.248	+1.122	
			771		
0	0	1	14.82	–0.345	
0	0	0	0.248	+1.121	
			808		
0	0	1	6.0	–0.323	$^{62}Ni_{0.765}Fe_{0.235}$, thermal neutron scattering[b,c]
0	¾	¾	1.5	–0.129	
0	½	1	1.3	–0.089	
0	0	½	0.75	+0.129	
			1273		
0	0	1	3.4	–0.444	$Ni_{0.775}Fe_{0.225}$, anomalous X-ray scattering[d,e]
0	½	1	1.3	–0.145	
0	0	0	0.6	+0.419	
0	0	½	0.75	+0.210	
0	0	1	2.0	–0.221	$Ni_{0.535}Fe_{0.465}$, anomalous X-ray scattering[e]
0	½	1	1.1	–0.040	
0	0	0	0.6	+0.294	
0	0	½	0.75	+0.147	
			753		
0	0	1	1.83	–0.127	$Fe_{0.632}Ni_{0.368}$, anomalous X-ray scattering[f]
0	½	1	1.2	–0.047	
0	0	0	0.4	+0.419	
0	0	½	0.95	+0.015	
			743		
0	0	1	1.45	–0.094	$Fe_{0.698}{}^{62}Ni_{0.302}$, thermal neutrons scattering[g]
0	½	1	1.2	–0.051	
0	0	½	1.0	0.000	
0	¾	¾	1.2	–0.051	

[a][110], [b][108], [c][109], [d][111], [e][113], [f][118], [g][119].

TABLE 6. The total (or 'paramagnetic') 'mixing' energies, $w_{\mathrm{tot(prm)}}(\mathbf{R}-\mathbf{R}', T_a)$, calculated with use of well-known approximations based on the radiation diffuse-scattering data for single-crystalline f.c.c.-Ni–Fe alloys at various annealing temperatures, T_a, and compositions, c_{Fe}.

	$l\ m\ n$	110	200	211	220	310	222	321	400	330	411
	No. of shells	I	II	III	IV	V	VI	VII	VIII	IX_l	IX_u
	$\lvert\mathbf{R}-\mathbf{R}'\rvert/a_0$	≈ 0.71	1	≈ 1.22	≈ 1.41	≈ 1.58	≈ 1.73	≈ 1.87	2	≈ 2.12	≈ 2.12
		$w_{\mathrm{tot(prm)}}(\mathbf{R}-\mathbf{R}', T_a)$ (meV)									
	$^{62}Ni_{0.765}Fe_{0.235}$ Permalloy										
958 K	KCM[a]	24.5	–6.68	2.4	1.66	–0.43	0.32	0.17	0.67	–0.31	0.4
	^{1}LIMCM[b]	32.0 (3.9)	–6.9 (2.1)	3.4 (1.5)	2.1 (1.2)	—	—	—	—	—	—
	^{2}LIMCM[b]	33.9 (2.2)	–5.3 (1.4)	4.1 (1.6)	1.7 (0.5)	—	—	—	—	—	—
	^{1}CFM[c]	61.8	–13.7	5.7	4.1	–1.0	0.7	0.4	1.6	–0.7	—
	SM[d]	58.3	–15.9	5.8	4.0	–1.0	0.7	0.4	1.6	–0.7	0.9
	^{1}GEM[d]	61.5	–13.4	5.8	—	—	—	—	—	—	—
	^{2}GEM[d]	62.0	—	—	—	—	—	—	—	—	—
808 K	KCM[a]	20.5	–9.72	0.82	0.27	0.17	–0.88	0.42	–0.1	–0.41	0.138
	^{1}LIMCM[b]	28.1 (7.3)	–10.6 (3)	0.5 (2.6)	–1.0 (2.2)	—	—	—	—	—	—
	^{2}LIMCM[b]	29.5 (3.8)	–9.1 (2.4)	2.6 (2.8)	0.0 (0.7)	—	—	—	—	—	—
	^{1}CFM[c]	59.5	–21.9	2.2	0.8	0.5	–2.3	1.2	–0.3	1.2	—
	our work	39.6	–4.7	6.2	–7.3	—	—	—	—	—	—
	SM[d]	55.8	–26.5	2.2	0.7	0.4	–2.3	1.2	–0.3	–1.2	0.3
	^{1}GEM[d]	59.5	–20.7	2.2	—	—	—	—	—	—	—
	^{2}GEM[d]	60.2	—	—	—	—	—	—	—	—	—
780 K	KCM[a]	21.3	–9.7	1.47	0.9	–0.75	–0.63	0.52	–0.31	0.28	–0.24
	^{1}LIMCM[b]	32.3 (3.5)	–9.4 (2.1)	2.6 (1.4)	0.8 (0.9)	—	—	—	—	—	—
	^{2}LIMCM[b]	32.9 (2.1)	–7.6 (1.3)	2.8 (1.6)	0.3 (0.4)	—	—	—	—	—	—
	^{1}CFM[c]	57.1	–20.5	3.6	2.3	–1.9	–1.6	1.3	–0.8	0.7	—
	^{2}CFM[c]	66.1	–19.7	3.8	2.5	–1.9	–1.6	1.3	–0.8	0.7	—
	^{3}CFM[c]	68.7	–19.4	3.9	2.5	–1.9	–1.6	1.3	–0.8	0.7	—
	SM[d]	53.6	–24.4	3.7	2.2	–1.8	–1.6	1.3	–0.8	0.7	–0.7
	^{1}GEM[d]	57.8	–17.8	3.7	—	—	—	—	—	—	—
	^{2}GEM[d]	58.6	—	—	—	—	—	—	—	—	—
776 K	^{1}LIMCM[b]	33.8 (2.9)	–11.1 (2)	3.7 (1.1)	2.2 (0.8)	—	—	—	—	—	—
	^{2}LIMCM[b]	34.9 (2.8)	–8.3 (1.7)	4.3 (2.1)	1.3 (0.5)	—	—	—	—	—	—
745 K	^{1}CFM[c]	61.3	–17.7	4.2	1.4	–2.2	–2.2	0.09	–1.8	–0.7	—
	SM[d]	57.2	–21.8	4.2	1.2	–2.2	–2.2	0.08	–1.8	–0.7	–0.4
	^{1}GEM[d]	61.8	–14.7	4.3	—	—	—	—	—	—	—
	^{2}GEM[d]	62.7	—	—	—	—	—	—	—	—	—
	$Ni_{0.775}Fe_{0.225}$ Permalloy at 1273 K										
	our work	49.1	–11.0	2.4	–13.5	—	—	—	—	—	—
	$Ni_{0.535}Fe_{0.465}$ Elinvar at 1273 K										
	our work	27.8	5.7	2.2	–10.5	—	—	—	—	—	—
	$Fe_{0.632}Ni_{0.368}$ Invar at 753 K										
	our work	15.1	–3.2	6.6	2.4	2.8	—	—	—	—	—
	$Fe_{0.698}{}^{62}Ni_{0.302}$ Invar at 743 K										
	our work	17.0	–5.0	5.3	3.9	—	—	—	—	—	—
	KCM[e]	2.81	–6.43	–0.77	–0.01	–0.32	–0.55	–0.08	–0.23	—	—
	^{1}CFM[c]	57.3	–12.6	–1.6	0	–0.6	–1.2	—	—	—	—
	^{2}CFM[c]	56.1	–12.5	–1.6	0	–0.6	–1.2	—	—	—	—
	^{3}CFM[c]	68.5	–12.7	–1.6	0	–0.6	–1.2	—	—	—	—

Continuation of Table 6.

[a][109], [b][120], [c][52], [d][57], [e][119].
SM—spherical model [39, 41, 42].
KCM—Krivoglaz–Clapp–Moss approximation [39–42, 109, 119].
LIMCM—Linearized Inverse Monte Carlo Method [120]: [1]LIMCM with 4 SRO parameters, α [109]; [2]LIMCM with 28 SRO parameters, α [109].
GEM—'gamma' expansion method [57]: [1]GEM and [2]GEM with $\Sigma_s = A\alpha^2$ and $\Sigma_s = A\alpha^2 + + B\alpha^3$, respectively.
CFM—Cluster Variation Field Method [50–52]: [1]CFM with $W_3^{nn} = 0$ meV; [2]CFM with $W_3^{nn} = -17.2$ meV; [3]CFM with $W_3^{nn} = -21.5$ meV (W_3^{nn}—three-particle potential value for nearest neighbours).

Let us consider experimental works of Goman'kov *et al.* [127, 128] based on the study of diffuse scattering of thermal neutrons by SRO of polycrystalline f.c.c.-Ni–Fe alloys. The Warren–Cowley SRO parameters for two coordination shells, α_n (n = I, II), deduced from experiments on polycrystalline samples of f.c.c.-Ni–Fe [127] alloys, and corresponding 'paramagnetic' 'mixing' energies, $w_{prm}(\mathbf{r}_{I,II})$, estimated by Rossiter and Lawrence [72] with using the KCM formula are presented in Table 7.

In Table 8, the same data are shown as a result of calculation provided for three coordination shells by Goman'kov *et al.* [128].

Let us briefly analyse the above-listed 'mixing' energies for f.c.c.-Ni–Fe alloys. Using the Fourier inversion, we have calculated dispersion dependences of Fourier components of total and 'paramagnetic' 'mixing' energies (5) for all h-s points and main symmetry directions within the irreducible region of the 1st *BZ* for some sets of interaction energies shown in Tables 6–8; see Figs. 7–10. One can see in Figs. 7–10 that Fourier components of 'mixing' energies obtained by different approaches (KCM [72, 109, 128], LIMCM [120] and CFM [52]) based on the diffuse scattering data (even extracted from scattering data for poly-

TABLE 7. 'Paramagnetic' contribution to 'mixing' energies for f.c.c.-Ni–Fe alloys at $T_a = 1273$ K, $w_{prm}(r_{I,II})$, calculated in [72] with use of both the KCM formula and the Warren–Cowley SRO parameters for two coordination shells obtained in neutron diffuse scattering experiments with polycrystalline samples of various compositions [127].

at.% Fe	$\alpha(r_I)$	$\alpha(r_{II})$	$w_{prm}(r_I)$ (meV)	$w_{prm}(r_{II})$ (meV)
25	–0.099	0.116	29	–33
30	–0.088	0.049	23	–13
50	–0.073	0.042	16	–9
60	–0.058	0.089	13	–20
65	–0.051	0.034	12	–8
70	–0.033	0.005	8	–1

TABLE 8. 'Paramagnetic' 'mixing' energies for f.c.c.-Ni–Fe alloys at T_a = = 1273 K, $w_{\text{prm}}\left(r_{\text{I,II,III}}\right)$, reported in [128] and calculated within the Cowley approximation using the Warren–Cowley SRO parameters for three coordination shells obtained in neutron diffuse scattering experiments with polycrystalline samples of various compositions.

at.% Fe	$w_{\text{prm}}\left(r_{\text{I}}\right)$ (meV)	$w_{\text{prm}}\left(r_{\text{II}}\right)$ (meV)	$w_{\text{prm}}\left(r_{\text{III}}\right)$ (meV)
18	42	8	9
22	53	5	10
25	38	−8	8
32	31	−9	5
37	16	−15	6
43	16	−14	5
50	14	−12	3
60	10	−10	3
65	9	−8	3
68	8	−5	3
70	5	−5	3
75	8	−11	3

crystalline samples) are in a good agreement with symmetry properties [25, 26, 86–88] of interatomic 'mixing' energies.

For instance, the global minimum of 'mixing' energy Fourier com-

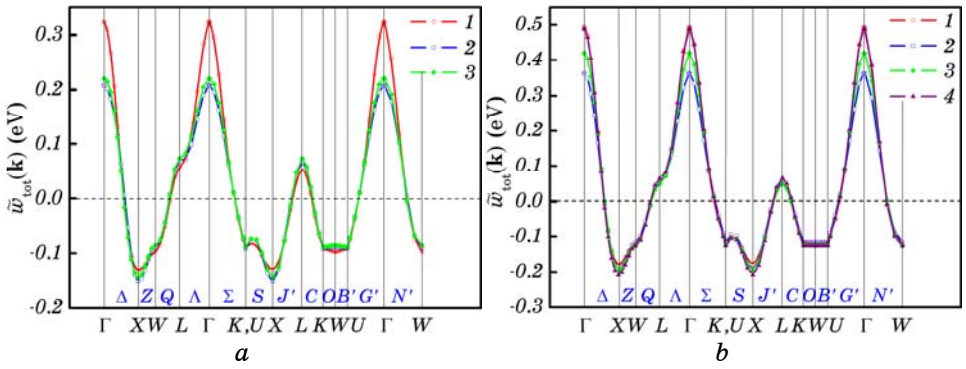

Fig. 7. Fourier components of total 'mixing' energies for the h-s points and main symmetry directions within the irreducible region of the 1st *BZ* for $Ni_{0.765}Fe_{0.235}$ Permalloy at different isothermal-annealing temperatures, $\tilde{w}_{\text{tot}}\left(\mathbf{k}, T_a\right)$, plotted using the KCM approximation [109] (*a*) (for T_a: *1*—958 K, *2*—808 K, *3*—780 K) and LIMCM method [120] (*b*) (for T_a: *1*—958 K, *2*—808 K, *3*—780 K, *4*—776 K) (see also Tables 5, 6).

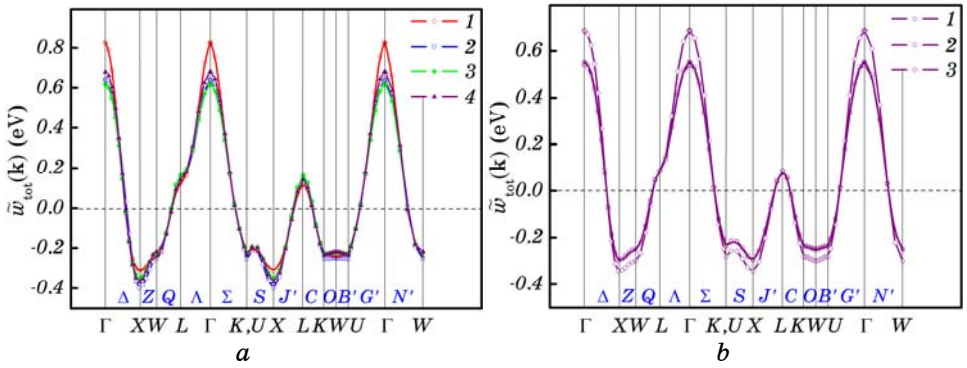

Fig. 8. Fourier components of total 'mixing' energies for the h-s points and main symmetry directions within the irreducible region of the 1st *BZ* for f.c.c.-Ni–Fe alloys at different isothermal-annealing temperatures, $\tilde{w}_{tot}(\mathbf{k}, T_a)$, plotted with use of the data presented in [52] for $Ni_{0.765}Fe_{0.235}$ (*a*) (using the CFM approximation with $W_3^{nn} = 0$ eV for T_a: *1*—958 K, *2*—808 K, *3*—780 K, *4*—745 K) and for $Fe_{0.698}Ni_{0.302}$ (*b*) (at $T_a = 743$ K with $W_3^{nn} = 0$ eV (*1*), –17.2 meV (*2*), –21.5 meV (*3*)) (see also Tables 5, 6).

ponents corresponds to the $X(0\ 0\ 1)$-type point of the 1st *BZ* surface that confirms a tendency to formation of the $L1_2$- or $L1_0$-type ordered structures. Distinction of the absolute values of 'mixing' energy Fourier components (especially, at the $X(0\ 0\ 1)$ or $\Gamma(0\ 0\ 0)$ points) is conditioned by both the applied approximations and the rough accuracy of used experimental data.

It is important to note that the 'mixing' energy Fourier component at the $X(0\ 0\ 1)$-type point decreases with increasing Fe content in f.c.c.-Ni–Fe alloys.

The majority of diffuse scattering experiments related to the SRO for f.c.c.-Ni–Fe alloys (see Tables 6–8 and Fig. 9, 10) were obtained for samples quenched from paramagnetic state of alloys. Therefore, for initial paramagnetic state of these alloys, it is necessary to use the replaced Fourier components, $\tilde{w}_{prm}(\mathbf{k}, T_a)$: $\tilde{w}_{tot}(\mathbf{k}, T_a) \to \tilde{w}_{prm}(\mathbf{k}, T_a)$ (with the exception of $Ni_{0.765}Fe_{0.235}$ alloy quenched from ferromagnetic region, T_a = = 808 K [109], which is describable by $\tilde{w}_{tot}(\mathbf{k}, T_a)$ from Eq. (15)).

Concentration dependences of the Fourier components of 'paramagnetic' 'mixing' energies for some quasi-wave vectors, namely, $\mathbf{k} = \mathbf{k}_X$, $\mathbf{k} \to \mathbf{k}_\Gamma$ and $\mathbf{k} = \mathbf{k}_\Gamma = \mathbf{0}$, are shown in Fig. 11, *a* and *b*. Dependences of $\tilde{w}_{prm}(\mathbf{0}, c_{Fe})$ and $\tilde{w}_{prm}(\mathbf{k} \to \mathbf{0}, c_{Fe})$ were fitted by the quadratic polynomials on concentration of Fe atoms, $c_{Fe} = c$, and for $\tilde{w}_{prm}(\mathbf{k}_X, c_{Fe})$, the linear polynomial was used (see Table 9). These assumptions can be justified by the revealed implicit concentration dependence of 'electrochemical' and 'strain-induced' interatomic-interaction contributions due to both the concentration dilatation of a lattice and the presence of

any inhomogeneities (and, in particular, long-wave fluctuations) of composition in f.c.c.-Ni–Fe alloys.

The value of Fourier component of 'paramagnetic' energies in Γ(0 0 0) point, $\tilde{w}_{\text{prm}}(\mathbf{0})$, was evaluated according to the following scheme. Considering isotropic character of 'electrochemical' 'mixing' energies, it is possible to write down:

$$\tilde{\varphi}_{\text{chem}}(\mathbf{0},c) \equiv \tilde{\varphi}_{\text{chem}}(\mathbf{k}\to\mathbf{0},c) \cong \left\langle \tilde{w}_{\text{prm}}(\mathbf{k}\to\mathbf{0},c)\big|_{\text{exp}} \right\rangle_{\mathbf{n}} - \left\langle \tilde{V}_{\text{si}}^{\text{FeFe}}(\mathbf{k}\to\mathbf{0},c) \right\rangle_{\mathbf{n}} \tag{40}$$

where $\left\langle \tilde{w}_{\text{prm}}(\mathbf{k}\to\mathbf{0},c)\big|_{\text{exp}} \right\rangle_{\mathbf{n}}$ is the average value of Fourier components of 'mixing' energies in paramagnetic state of an alloy, which are estimated by the KCM formula (36) using the experimental data on diffuse scattering intensities for $\mathbf{k}\to\mathbf{0}$ along those directions, $\mathbf{n}=\mathbf{k}/k$, accessible in experiments reported in [108–119] (see also Tables 5 and 6); $\left\langle \tilde{V}_{\text{si}}^{\text{FeFe}}(\mathbf{k}\to\mathbf{0},c) \right\rangle_{\mathbf{n}}$ is the averaged value of the calculated Fourier components of 'strain-induced' interaction energies for $\mathbf{k}\to\mathbf{0}$ along all directions, $\mathbf{n}=\mathbf{k}/k$, in particular, as shown in Fig. 4; $\langle\ldots\rangle_{\mathbf{n}}$ is an average over all directions, $\mathbf{n}=\mathbf{k}/k$, along $\mathbf{k}\to\mathbf{0}$ within the reciprocal space. Then, according to the definition in Eq. (15),

$$\tilde{w}_{\text{prm}}(\mathbf{0},c) \cong \tilde{\varphi}_{\text{chem}}(\mathbf{0},c) + \tilde{V}_{\text{si}}^{\text{FeFe}}(\mathbf{0},c), \tag{41}$$

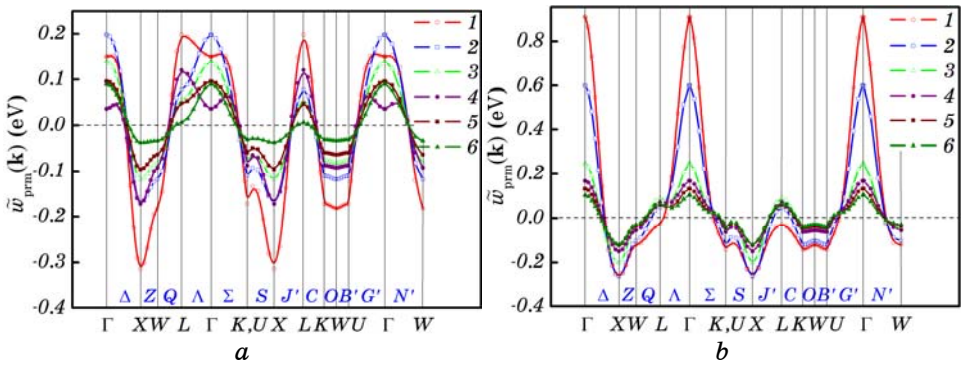

Fig. 9. Fourier components of 'paramagnetic' 'mixing' energies, $\tilde{w}_{\text{prm}}(\mathbf{k}, c_{\text{Fe}})$, for the h-s points and main symmetry directions within the irreducible region of the 1st *BZ* for f.c.c.-Ni–Fe alloys at different concentrations of Fe atoms, c_{Fe}. Diffuse scattering experiments have been done for polycrystalline samples. (*a*): *1*—$Ni_{0.75}Fe_{0.25}$, *2*—$Ni_{0.7}Fe_{0.3}$, *3*—$Ni_{0.5}Fe_{0.5}$, *4*—$Ni_{0.4}Fe_{0.6}$, *5*—$Ni_{0.35}Fe_{0.65}$, *6*—$Ni_{0.3}Fe_{0.7}$ (for all alloys, T_a = 1273 K); the evaluations were done with use of data from Table 7 and [72]. (*b*): *1*—$Ni_{0.78}Fe_{0.22}$, *2*—$Ni_{0.75}Fe_{0.25}$, *3*—$Ni_{0.63}Fe_{0.37}$, *4*—$Ni_{0.5}Fe_{0.5}$, *5*—$Ni_{0.4}Fe_{0.6}$, *6*—$Ni_{0.25}Fe_{0.75}$; the evaluations were made with use of data from Table 8 and [128].

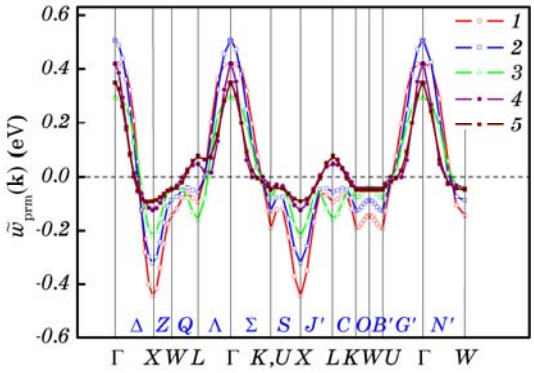

Fig. 10. Fourier components of 'paramagnetic' 'mixing' energies, $\tilde{w}_{\rm prm}(\mathbf{k})$, for the h-s points and main symmetry directions within the irreducible region of the 1st *BZ* for f.c.c.-Ni–Fe alloys at different isothermal-annealing temperatures, T_a, and concentrations of Fe atoms, $c_{\rm Fe}$. *1*—$Ni_{0.775}Fe_{0.225}$ at $T_a = 1273$ K, *2*—$Ni_{0.765}Fe_{0.235}$ at $T_a = 808$ K, *3*—$Ni_{0.535}Fe_{0.465}$ at $T_a = 1273$ K, *4*—$Fe_{0.632}Ni_{0.368}$ at $T_a = 753$ K, *5*—$Fe_{0.698}Ni_{0.302}$ at $T_a = 743$ K. The evaluations were carried out by the data presented in Table 6 for single-crystal diffraction data according to [108–119].

the Fourier component of 'paramagnetic' 'mixing' energies, $\tilde{w}_{\rm prm}(\mathbf{0},c)$, for 'fundamental' reciprocal-space point, $\mathbf{k}_\Gamma$, was estimated.

Exactly so, the 'paramagnetic' 'mixing' energy Fourier components,

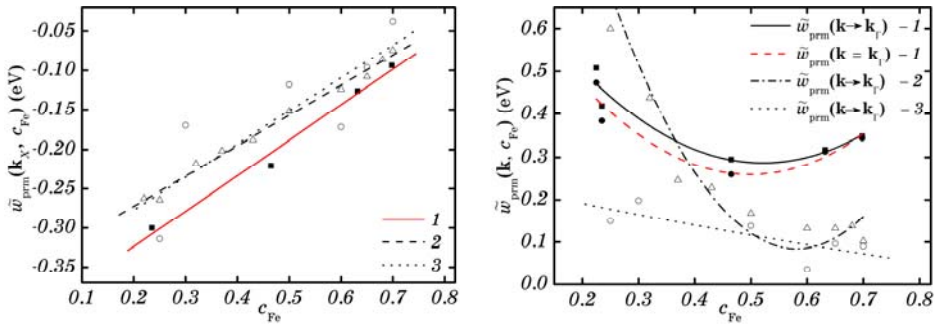

Fig. 11. Concentration dependences of Fourier components of 'paramagnetic' 'mixing' energies, $\tilde{w}_{\rm prm}(\mathbf{k},c_{\rm Fe})$, for some quasi-wave vectors within the 1st *BZ*, $\mathbf{k} = \mathbf{k}_X$ (*a*), $\mathbf{k} = \mathbf{0}$ and $\mathbf{k} \xrightarrow[\mathbf{k}\downarrow\uparrow\mathbf{k}_X]{} \mathbf{0}$ (*b*), for f.c.c.-Ni–Fe alloys. ○, △, ■—data in Fig. 9(*a*), (*b*) and Fig. 10, respectively. ●—results of calculation by Eqs. (40), (41). Lines—polynomials specified by coefficients from the Table 9, where the energy Fourier components are fitted to the data of diffuse scattering experiments for: *1*—single crystals and *2*, *3*—polycrystals (in accordance with [108–119] and [128, 72], respectively).

$\tilde{w}_{\text{prm}}(\mathbf{k},c)$, have been evaluated for some quasi-wave vectors, $\mathbf{k}=\mathbf{k}_X$, $\mathbf{k}\to\mathbf{0}$ and $\mathbf{k}=\mathbf{0}$, in a certain concentration region. Their concentration dependences were fitted by the polynomials of 1st or 2nd degree with coefficients presented in Table 9 and are plotted in Fig. 11, *a* and *b*.

In Figures 11, *a* and *b*, it is evident that Fourier components of 'paramagnetic' 'mixing' energies for *X*-star of ordering quasi-wave vector, $\tilde{w}_{\text{prm}}(\mathbf{k}_X,c_{\text{Fe}})$, estimated with the KCM formula (36) are well satisfactorily described by linear dependence on concentration of Fe atoms, c_{Fe}, while $\tilde{w}_{\text{prm}}(\mathbf{k}\to\mathbf{0},c_{\text{Fe}})$ and $\tilde{w}_{\text{prm}}(\mathbf{0},c_{\text{Fe}})$ obey quadratic law. The magnitudes of $\tilde{w}_{\text{prm}}(\mathbf{k}_X,c_{\text{Fe}})$ evaluated from diffuse scattering data for polycrystalline samples are lower than the same obtained from diffraction experiments with the single crystals. Though the inclinations of linear concentration dependences of $\tilde{w}_{\text{prm}}(\mathbf{k}_X,c_{\text{Fe}})$ for the ordering *X*-star are almost identical, but in the vicinity of Γ point, the inclinations of quadratic concentration dependences of $\tilde{w}_{\text{prm}}(\mathbf{k}\to\mathbf{0},c_{\text{Fe}})$ and $\tilde{w}_{\text{prm}}(\mathbf{0},c_{\text{Fe}})$ differ considerably with each other. It is conditioned by considering only 2–3 coordination shells in the interatomic-interaction potentials evaluated in [72, 128], and, for polycrystalline samples, by boundedness of the separation method for diffuse scattering component caused by SRO, $I_{\text{SRO}}(\mathbf{k})$, *etc*. (The detailed analysis of available methods for determination of diffuse scattering intensities can be found in an outstanding review by Schönfeld [129]; see also full list of references therein.) Therefore, in our calculations, we have used the Fourier components of 'paramagnetic' 'mixing' energies estimated on the basis of an analysis of the diffuse scattering patterns from single crystals only (see 1st and 3rd lines in Table 9).

TABLE 9. Coefficients of concentration dependences of the 'paramagnetic' 'mixing' energy Fourier components, $\tilde{w}_{\text{prm}}(\mathbf{k},c)$, roughly described by the 1st- or 2nd-degree polynomials, b_0+b_1c or $b_0+b_1c+b_2c^2$, for f.c.c.-Ni–Fe alloys and obtained by fitting the estimated diffuse scattering data taken from Figs. 9(*a*), (*b*) and 10.

Quasi-wave vectors	b_0 (eV)	b_1 (eV)	b_2 (eV)	Mean-square deviation, R^2	Fitting	Comments
0 0 1	–0.414	0.450	—	0.986	1st degree	Extracted from single-crystal data [108–119]
$h\,k\,l\to 0\,0\,0$	0.855	–2.177	2.087	0.900	2nd degree	
0 0 0	0.843	–2.339	2.344	0.916	2nd degree	
0 0 1	–0.361	0.419	—	0.694	1st degree	Extracted from polycrystal data [72]
$h\,k\,l\to 0\,0\,0$	0.248	–0.296	0.065	0.611	2nd degree	
0 0 1	–0.349	0.384	—	0.995	1st degree	Extracted from polycrystal data [128]
$h\,k\,l\to 0\,0\,0$	1.929	–6.344	5.453	0.944	2nd degree	

The total 'mixing' energies strongly depend on temperature in temperature–concentration region of magnetic alloy due to the strong temperature dependence of their magnetic contributions such as $\tilde{w}_{\text{mag}}(\mathbf{k}, c, T)$. For instance, by solving transcendental set of Eq. (21), for the $Ni_{0.765}Fe_{0.235}$ alloy within the temperature interval of its magnetic state with atomic SRO state only, $T_K < T < T_C$, it is possible to plot the temperature dependence of Fourier component of total 'mixing' energies for the ordering $X(0\,0\,1)$-type star of quasi-wave vector, $\tilde{w}_{\text{tot}}(\mathbf{k}_X, c, T)$ (15); see Fig. 12. The values of $\tilde{w}_{\text{tot}}(\mathbf{k}_X, c, T)$ estimated with the KCM formula (36), using the diffuse scattering intensities as reported by Bley *et al.* [110] (see Table 5) are also presented for comparison in Fig. 12.

As shown in Fig. 12, the temperature dependence of $\tilde{w}_{\text{tot}}(\mathbf{k}_X, c, T)$ estimated with the KCM formula using the diffuse scattering data reported in [110], approaching to the order–disorder phase transformation temperature, T_K, deviates from the $\tilde{w}_{\text{tot}}(\mathbf{k}_X, c, T)$ dependence on T calculated with (15). Such a distinction is generally due to the increase of amplitudes of the concentration heterogeneity fluctuations (and thereupon concentration waves) in the vicinity of this point of phase transformation of the 1st kind. In the consequence, these effects manifest themselves in diffuse scattering intensity, $I_{\text{SRO}}(\mathbf{k}_X, c, T)$, resulted in [110] (see Table 5). Only above T_K by 15–20 K, both evaluations coincide (see, for example, the similar effect close to the order–disorder phase transformation temperature for Cu_3Au alloy as report-

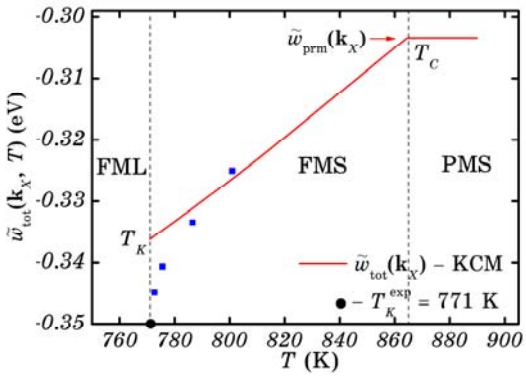

Fig. 12. Temperature dependence of Fourier component of total 'mixing' energies for the ordering X-star, $\tilde{w}_{\text{tot}}(\mathbf{k}_X, c, T)$, in the region of ferromagnetic state (FMS) of $Ni_{0.765}Fe_{0.235}$ Permalloy with atomic SRO only. ■— $\tilde{w}_{\text{tot}}(\mathbf{k}_X, c, T)$ estimated with the KCM formula (36) using the diffraction data [110]. Solid line— $\tilde{w}_{\text{tot}}(\mathbf{k}_X, c, T)$ calculated with (15) solving (21). FML, PMS—the ferromagnetic atomic-LRO and paramagnetic atomic-SRO regions, respectively. In our calculation, the 'exchange' 'integrals', $\tilde{J}_{\alpha\alpha'}(\mathbf{k})$, were specified for $s_{\text{Ni}} = 1/2$ and $s_{\text{Fe}} = 3/2$ (see Table 1).

ed by Chen and Cohen [130]). It is obvious that, at the order–disorder phase transformation point precisely, T_K, there is a jump of total 'mixing' energy arising due to the jump of magnetic-energy contribution conditioned by the jump of atomic LRO parameter under the 1st kind phase transition: $\Delta\sigma_{\mathrm{Ni,Fe}}(\Delta\eta)|_{T=T_K} \neq 0$ (see also Eq. (21)). On the other hand, under transition from ferromagnetic state with atomic SRO only (FMS) to ferromagnetic state with atomic LRO (FML), T-dependence of $\tilde{w}_{\mathrm{tot}}(\mathbf{k}_X, c, T)$ will change its inclination. In the PMS region, $T > T_C$, total 'mixing' energies consist of 'paramagnetic' contributions only, and $\tilde{w}_{\mathrm{tot}}(\mathbf{k}_X, c, T) = \tilde{w}_{\mathrm{prm}}(\mathbf{k}_X, c, T)$ does not almost depend on temperature (if the 'strain-induced' contribution, $\tilde{V}_{\mathrm{si}}^{\mathrm{FeFe}}(\mathbf{k}, T)$, manifests a weak temperature dependence; see section 3.3 and Fig. 6). It should be mentioned that the presentation of the total 'mixing' energy for a binary alloy with two 'magnetic' constituents in the form of Eq. (15) explains simply the nature of both temperature (see Fig. 6 and 12) and concentration (see Fig. 5) dependences (within the assumption of the effectively 'pair-wise' interatomic interactions only). If we consider explicitly a mutual influence of the magnetic and atomic subsystems in the configuration-dependent part of free energy of a disordered alloy (see Eqs. (19)–(22)), the KCM formula (36) stays valid [131], and it is not necessary to overestimate the statistical correlation influence and many-particle force interactions of substitutional atoms in magnetic alloy, at the same time, unreasonably neglecting the apparent magnetism of an alloy [50–52, 57].

Finally, we would like to note that, at low temperatures close to 0 K, the 'magnetic' 'mixing'-energy contribution will be perceptibly high with respect to 'paramagnetic' one (see Eq. (15) and Tables 1, 2, 9). In this case, we should consider the microheterogeneous magnetic-moment state effects, itinerant-magnetism contribution, and their interrelations with static local lattice-distortion fields. One of the examples of such microheterogeneous states was mentioned in articles by Ono *et al.* [132] and Tsunoda *et al.* [133]. Here, by means of anomalous X-ray [132] and thermal neutron [133] diffuse-scattering investigations of Fe–Ni Invar, the authors found a few anomalies of intensity behaviour close to the Bragg points in reciprocal space. They made conclusion that such anomalies are due to the formation of Fe-rich clusters with a lattice deformation consisting of a shear wave propagating along the $\langle 1\,1\,0 \rangle$ direction that is the appearance of premartensitic embryos with a lattice deformation toward the 'low-temperature' f.c.c.–b.c.c. martensitic transformation of Fe–Ni alloys. Indeed, when the temperature is decreased, the thermal diffuse-scattering contributions of one-, two-, and many-phonon effects in the total diffuse-scattering intensities are decreased as well [129]. The elastically anisotropic 'strain-induced' interatomic-interaction energy contribution will act the significant part in a pattern of diffuse-scattering intensities then

(see Eqs. (15), (31), (32) and the KCM formula (36)). As a result, the orientational (azimuthal) dependence of diffuse-scattering intensities around the Bragg reflections (in the vicinity of 'fundamental' point $\Gamma(0\,0\,0)$) will be pronounced effect [131] (see also Fig. 4 and 6). At the intermediate and elevated temperatures, such phenomena will disappear, and intensities become more isotropic.

4. CONCLUSION

In a given article, the statistical-thermodynamic model for f.c.c. binary substitutional alloys with two magnetic constituents has been considered by the example of f.c.c.-Ni–Fe alloys. Based on the sets of independent diffraction (coherent and diffuse scattering) and magnetic measurements for dis(ordered) f.c.c.-Ni–Fe alloys, the careful reciprocal-space analysis of interatomic interactions (including different contributions of the various nature) and their temperature-concentration dependences have been carried out in detail.

In section 2, within the scope of the SCF and MF approximations, using the SCW method, the statistical-thermodynamic model for f.c.c. substitutional alloys with two magnetic constituents has been developed. We have considered the analytical expressions for configuration-dependent parts of thermodynamic potentials for macroscopically homogeneous atomic-LRO phases of $L1_2$-Ni_3Fe-, $L1_0$-NiFe- and $L1_2$-Fe_3Ni-types. Thereby, configuration-dependent parts of internal energy and entropy contributions for both the magnetic and atomic subsystems have been analysed (Eqs. (8)–(13), (17)). As shown, the total configuration-dependent parts of free energies for mentioned structural types depend on the LRO parameters of both the atomic and magnetic subsystems (subjected to their strong interrelations) as well as on the temperature and composition (see Eqs. (19)–(22)).

In subsection 3.1, within the scope of the MSCF approximation, using the available experimental data on magnetic phase-transition temperature dependence on concentration of Fe atoms, $T_C(c_{Fe})$, we have estimated the 'exchange' 'integrals' for magnetic interactions between the atomic moments in f.c.c.-Ni–Fe alloys in both direct and reciprocal space representations. Pair-wise 'exchange' 'integrals', $J_{NiNi}(r_I)$ and $J_{NiFe}(r_I)$, correspond to ferromagnetic interactions in Ni–Ni and Ni–Fe pairs of neighbouring atoms, respectively, and $J_{FeFe}(r_I)$ corresponds to antiferromagnetic Fe–Fe interatomic interaction (see Tables 1, 2) that may result in frustrations of magnetic and composition orders.

In subsection 3.2, we have analyzed well-known 'electrochemical' interatomic-interaction energies for f.c.c.-Ni–Fe alloys, which were reported in the scientific publications. As shown here, the central unsatisfactory feature of these energies is the limitation of interaction extension in space only to the 1st nearest neighbour distances that is

too rough approximation for the real metallic alloys (in particular, f.c.c.-Ni–Fe). Besides, available 'electrochemical' interatomic-interaction energy parameters are often inconsistent with symmetry properties of total 'mixing' energies [25, 26, 86–88].

In subsection 3.3, on the basis of the Matsubara–Kanzaki–Krivoglaz lattice-statics method, the 'concentration' and temperature dependences of 'strain-induced' interaction parameters for Ni and Fe atoms dissolved in solid solutions based on the f.c.c. γ-Fe and α-Ni host-crystal lattices, respectively, have been calculated. As shown, the 'strain-induced' interaction energies significantly differ for Permalloy and Invar compositions, decreasing modulo with increase of Fe atomic concentration, c_{Fe}. One can note that 'strain-induced' interaction energy Fourier components increase with the temperature increasing and obey the linear law (for solutions based on α-Ni) for all h-s points, including Γ(0 0 0), but their changes are not significant and make up 10% only (with respect to their values at $T = 0$ K) within the temperature interval of 0–1000 K. Thus, in a whole considered 'T–c_{Fe}' region, the 'strain-induced' interaction energies are long-range, 'quasi-oscillating' and orientation-dependent functions of interatomic relative-position vectors. As revealed (see Fig. 4), the 'strain-induced' interaction energy Fourier component is a non-analytical function at the Γ(0 0 0) point precisely, which follows the leftmost inequality Eq. (34) (see also [37, 85, 98]) for finite crystals (with a stress-free surface) containing the interacting point defects. The last-named property was erroneously understood often by a number of authors (see, for example, [62, 104, 134]) that led them to both the misinterpretation of 'non-analytical behaviour' of reciprocal-space parameters of interactions between point defects in host crystals and the incorrect processing of available experimental data on the diffuse scattering of radiations in (dis)ordered alloys. (In other words, the 'non-analyticity' of 'strain-induced' interaction between point defects in finite crystals does not identical with its directionality owing to both the crystalline anisotropy and the elastic anisotropy.)

In subsection 3.4, within the scope of the SCF approximation, using the Krivoglaz–Clapp–Moss formula for available experimental data on the elastic diffuse scattering of radiations (X-rays or thermal neutrons) by SRO in poly- and single-crystalline samples of f.c.c.-Ni–Fe alloys, within the assumption of the effectively 'pair-wise' interatomic interaction only, we have calculated the total and 'paramagnetic' 'mixing' energies. As revealed, the Fourier components of 'paramagnetic' 'mixing' energies, $\tilde{w}_{\mathrm{prm}}\left(\mathbf{k},c_{\mathrm{Fe}}\right)$, are implicitly but strongly dependent on concentration of Fe atoms (see Table 9) due to direct 'electrochemical' interactions of Ni and Fe atoms at the sites of f.c.c. lattice liable to concentration dilatations. For the h-s X(0 0 1)-type points of the 1$^{\mathrm{st}}$ BZ surface, this dependence is virtually linear, and for the Bragg 'struc-

tural' ('fundamental') point $\Gamma(0\ 0\ 0)$, this dependence mainly obeys a parabolic profile with a minimum in Invar composition region ($c_{\mathrm{Fe}} \cong$ $\cong 0.55$–0.7). Seemingly, the last-described dependence is conditioned by the competition between short-range 'electrochemical' and long-range 'strain-induced' contributions in 'paramagnetic' interatomic interactions that may release the fluctuations (including long-wave ones) of frustrated 'bonds' between the magnetic moments of Fe (and even Ni) atoms (in Invar composition region especially) interplaying with their static concentration waves and (or) with the static crystal-lattice distortion waves by way of the concurrent formation of magnetic and atomic heterogeneities in Invar at issue on the microscopic and nanoscale levels. Besides, the relevant combination of Fourier components of 'exchange' 'integrals', $\{\tilde{J}_{\alpha\alpha'}(\mathbf{k}_X)\}$, such as $\tilde{w}_{\mathrm{mag}}(\mathbf{k}_X)$ in Eq. (15), demonstrate the same sign (see subsection 3.1) as respective 'paramagnetic' parameter, $\tilde{w}_{\mathrm{prm}}(\mathbf{k}_X)$. Therefore, for magnetic regions of a solid solution, the depth of a negative global minimum of total 'mixing' energy Fourier component, $\tilde{w}_{\mathrm{tot}}(\mathbf{k}_X)$, for the $X(0\ 0\ 1)$-type star of quasi-wave vector (generating an atomic ordering) increases that testifies a growth of the SRO and LRO states in atomic configurations.

In addition, we have calculated the temperature dependence of total 'mixing' energies of an alloy, and, as shown, the temperature dependence of $\tilde{w}_{\mathrm{tot}}(\mathbf{k},T)$ is mainly caused by the strong temperature dependence of 'magnetic' 'mixing'-energy contribution, $\tilde{w}_{\mathrm{mag}}(\mathbf{k},T)$ (see Fig. 12 and Eq. (15)). Therefore, before explanation of microstructure features and microscopic physical phenomena [1–4, 108–119, 135–137] in magnetic alloy at issue, it is necessary to investigate an essential interplay of the atomic and magnetic orders of constituents, and it may be found that there is no need for considering both the substitutional correlation between atoms and their many-particle force interactions [50–52, 57].

ACKNOWLEDGEMENT

The authors express their appreciation to Dr. H. M. Zapolsky, Prof. D. Blavette and Prof. D. Ledue (GPM, UMR 6634 CNRS, Université de Rouen, France) for very constructive discussion of the results obtained in the course of a given work. One of the authors (S. M. B.) acknowledges the partial financial assistance he has received from GPM (Rouen, France) as well as Nanoscience Foundation (Grenoble, France). We thank Prof. M. S. Blanter (Moscow State Academy of Instrumental Engineering and Information Science, Russia), Dr. R. V. Chepulskii (Duke University, U.S.A.), Prof. B. Schönfeld (ETH, Laboratory of Metal Physics and Technology, Switzerland), Dr. G. E. Ice (Oak Ridge National Laboratory, U.S.A.) and Mr. D. Pavlyuchkov (Forschungszentrum Jьlich GmbH, Germany) for kindly providing their publications

and communicating important references. We apologize to other researchers, which have actively worked on the various problems related with our work, whose relevant publications are not referenced and discussed in a given paper because of volume limitations. This work has been inspired by discussions at the several congresses and conferences, primarily, European Congress on Advanced Materials and Processes 'EUROMAT2007' (10–13 Sept. 2007, Nürnberg, FRG), 'Contemporary Problems of Metal Physics' (7–9 Oct. 2008, Kyyiv, Ukraine), *etc*.

REFERENCES

1. A. P. Miodownik, *Physics and Applications of Invar Alloys*. *Honda Memorial Series on Materials Science*, No. 3 (Eds. H. Saito et al.) (Tokyo: Maruzen Company, Ltd.: 1978), chap.12, p. 288.
2. G. Béranger, F. Duffaut, J. Morlet, and J.-F. Tiers, *Les Alliages De Fer et De Nickel. Cent ans aprus la découverte de l'Invar...* (Londres–Paris–New York: Technique & Documentation: 1996).
3. V. L. Sedov, *Antiferromagnetism of γ-Fe. Problem of Invar* (Moscow: Nauka: 1987) (in Russian).
4. L. J. Swartzendruber, V. P. Itkin, and C. B. Alcock, *J. Phase Equil.*, **12**: 288 (1991).
5. G. Cassiamani, J. de Keyzer, R. Ferro, U. E. Klotz, J. Lacaze, and P. Wollants, *Intermetallics*, **14**: 1312 (2006).
6. J. Crangle and G.C. Hallam, *Proc. Roy. Soc. A*, **272**: 119 (1963).
7. C. E. Johnson, M. S. Ridout, and T. E. Cranshaw, *Proc. Phys. Soc.*, **81**: 1079 (1963).
8. W. L. Wilson and R. W. Gould, *J. Appl. Crystallogr.*, **5**: 125 (1972).
9. T. G. Kollie and C. R. Brooks, *Phys. Stat. Sol. A*, **19**: 545 (1973).
10. J. W. Cable and E. O. Wollan, *Phys. Rev. B*, **7**: 2005 (1973).
11. J. W. Drijver, F. van der Woude, and S. Radelaar, *Phys. Rev. B*, **16**: 985 (1977).
12. J. W. Drijver, F. van der Woude, and S. Radelaar, *Phys. Rev. B*, **16**: 993 (1977).
13. J.-P. Simon, O. Lyon, F. Faudot, L. Boulanger, and O. Dimitrov, *Acta Metall. Mater.*, **40**: 2693 (1992).
14. P. R. Munroe and M. Hatherly, *Scripta Metall. Mater.*, **32**: 93 (1995).
15. T. Horiuchi, M. Igarashi, F. Abe, and T. Mohri, *Calphad*, **26**: 591 (2002); T. Mohri and Y. Chen, *J. Alloys and Compounds*, **383**: 23 (2004); Y. Chen, S. Iwata, and T. Mohri, *Rare Metals*, **25**: 437 (2006); T. Mohri, Y. Chen, and Y. Jufuku, *Calphad*, **33**: 244 (2009).
16. V. Crisan, P. Entel, H. Ebert et al., *Phys. Rev. B*, **66**: 014416-1 (2002).
17. Y. Mishin, M. J. Mehl, and D. A. Papaconstantopoulos, *Acta Mater.*, **53**: 4029 (2005).
18. I. A. Abrikosov, O. Eriksson, P. Söderlind, H. L. Skriver, and B. Johansson, *Phys. Rev. B*, 51: 1058 (1995).
19. M. van Schilfgaarde, I. A. Abrikosov, and B. Johansson, *Nature*, **400**: 46 (1999).
20. F. Liot, S. I. Simak, and I. A. Abrikosov, *J. Appl. Phys.*, **99**: 08P906 (2006).
21. I. A. Abrikosov, F. Liot, T. Marten, and E. A. Smirnova, *J. Magn. Magn. Mater.*, **300**: 211 (2006).
22. I. A. Abrikosov, A. E. Kissavos, F. Liot et al., *Phys. Rev. B*, **76**: 014434-1 (2007).
23. C. Asker, L. Vitos, and I. A. Abrikosov, *Phys. Rev. B*, **79**: 214112-1 (2009).
24. F. Liot and I. A. Abrikosov, *Phys. Rev. B*, **79**: 014202-1 (2009).

25. A. G. Khachaturyan, *Prog. Mat. Sci.,* **22**: 1 (1978).
26. A. G. Khachaturyan, *Theory of Structural Transformations in Solids* (New York: John Wiley & Sons: 1983).
27. D. de Fontaine, *Solid State Physics*, vol. **34** (Eds. H. Ehrenreich, F. Seits, and D. Turnbull) (New York: Academic Press: 1979), p. 73.
28. M. A. Krivoglaz and A. A. Smirnov, *The Theory of Order–Disorder in Alloys*, (London: Macdonald: 1969).
29. F. Ducastelle, *Order and Phase Stability in Alloys* (New York: Elsevier: 1991).
30. M. A. Krivoglaz, *X-Ray and Neutron Diffraction in Nonideal Crystals* (Berlin: Springer: 1996); M. A. Krivoglaz, *Diffuse Scattering of X-Rays and Thermal Neutrons by Fluctuational Inhomogeneities of Imperfect Crystals* (Berlin: Springer: 1996).
31. V. M. Danilenko and A. A. Smirnov, *Fiz. Met. Metalloved.*, **14**: 337 (1962) (in Russian).
32. V. M. Danilenko, D. R. Rizdvyanetskii, and A. A. Smirnov, *Fiz. Met. Metalloved.*, **15**: 194 (1963) (in Russian).
33. V. M. Danilenko, D. R. Rizdvyanetskii, and A. A. Smirnov, *Fiz. Met. Metalloved.*, **16**: 3 (1963) (in Russian).
34. S. V. Semenovskaya, *Phys. Stat. Sol. B*, **64**: 291 (1974).
35. G. Inden, *Physica B*, **103**: 82 (1981).
36. V. A. Tatarenko, T. M. Radchenko, and V. M. Nadutov, *Metallofiz. Noveishie Tekhnol.*, **25**: 1303 (2003) (in Ukrainian); V. A. Tatarenko and T. M. Radchenko, *Intermetallics*, **11**: 1319 (2003); T. M. Radchenko and V. A. Tatarenko, *Uspehi Fiziki Metallov*, **9**: 1 (2008) (in Ukrainian).
37. S. M. Bokoch and V. A. Tatarenko, *Solid State Phenomena*, **138**: 303 (2008); V. A. Tatarenko, S. M. Bokoch, V. M. Nadutov et al., *Def. Diff. Forum*, **280–281**: 29 (2008).
38. J. S. Smart, *Effective Field in Theories of Magnetism* (Philadelphia–London: W. B. Saunders Company: 1966).
39. M. A. Krivoglaz, *Zh. Eksp. Teor. Fiz.*, **32**: 1368 (1957) (in Russian).
40. P. C. Clapp and S. C. Moss, *Phys. Rev.*, **142**: 418 (1966).
41. P. C. Clapp and S. C. Moss, *Phys. Rev.*, **171**: 754 (1968).
42. P. C. Clapp and S. C. Moss, *Phys. Rev.*, **171**: 764 (1968).
43. V. Gerold and J. Kern, *Acta Metall.*, **35**: 393 (1987).
44. R. V. Chepulskii and V. N. Bugaev, *J. Phys.: Condens. Matter*, **10**: 7309 (1998).
45. I. R. Yukhnovskii and Z. A. Gurskii, *Quantum Statistical Theory of Disordered Systems* (Kiev: Naukova Dumka: 1991) (in Russian).
46. B. L. Gyorffy and G. M. Stocks, *Phys. Rev. Lett.*, **50**: 374 (1983).
47. J. B. Staunton and B. L. Gyorffy, *Phys. Rev. Lett.*, **69**: 371 (1992).
48. J. B. Staunton, D. D. Johnson, and F. J. Pinski, *Phys. Rev. B*, 50: 1450 (1994).
49. R. A. Tahir-Kheli, *Phys. Rev.*, **188**: 1142 (1969).
50. V. G. Vaks, N. E. Zein, and V. V. Kamyshenko, *J. Phys. F: Met. Phys.*, **18**: 1641 (1988).
51. V. G. Vaks, N. E. Zein, and V. V. Kamyshenko, *J. Phys.: Condens. Matter*, **1**: 2115 (1989).
52. V. G. Vaks and V. V. Kamyshenko, *J. Phys.: Condens. Matter*, **3**: 1351 (1991).
53. R. Kikuchi, *Phys. Rev.*, **81**: 988 (1951); D. de Fontaine and R. Kikuchi, *US Natl. Bur. Stand. Publ.* (SP–496) (1977), p. 999.
54. D. de Fontaine, *Solid State Physics*, vol. **47** (Eds. H. Ehrenreich and D. Turn-

bull) (New York: Academic Press: 1994), p. 33.
55. A. Finel, *Statics and Dynamics of Alloy Phase Transformations*, NATO Advanced Studies Institute, Series B: Physics, vol. **319** (Eds. P. E. A Turchi and A. Gonis) (New York: Plenum: 1994), p. 495.
56. J. M. Sanchez, V. Pierron-Bohnes, and F. Mejía-Lira, *Phys. Rev. B*, **51**: 3429 (1995).
57. V. I. Tokar, I. V. Masanskii, and T. A. Grishchenko, *J. Phys.: Condens. Matter*, **2**: 10199 (1990); I. V. Masanskii, V. I. Tokar, and T. A. Grishchenko, *Phys. Rev. B*, **44**: 4647 (1991).
58. I. Tsatskis, *Phil. Mag. Lett.*, **78**: 403 (1998); I. Tsatskis, *J. Phys.: Condens. Matter*, **10**: L145 (1998); I. Tsatskis and E. K. H. Salje, *J. Phys.: Condens. Matter*, **10**: 3791 (1998); I. Tsatskis, *Phys. Letters A*, **241**: 110 (1998). (Former name of I. Tsatskis was I.V. Masanskii as quoted in [57].)
59. R. V. Chepulskii, *Phys. Rev. B*, **69**: 134431-1 (2004); R. V. Chepulskii, *Phys. Rev. B*, **69**: 134432-1 (2004).
60. V. N. Bugaev, H. Reichert, O. Shchyglo et al., *Phys. Rev. B*, **65**: 180203(R)-1 (2002).
61. A. Udyansky, V. N. Bugaev, W. Schweika et al., *Phys. Rev. B*, **71**: 140201(R)-1 (2005).
62. O. Shchyglo, V. N. Bugaev, R. Drautz et al., *Phys. Rev. B*, **72**: 140201(R)-1 (2005).
63. V. N. Bugaev, A. Udyansky, O. Shchyglo, H. Reichert, and H. Dosch, *Phys. Rev. B*, **74**: 024202-1 (2006).
64. E. P. Wohlfarth, *J. Phys. C*, **2**: 68 (1969).
65. E. I. Kondorsky, *Zh. Eksp. Teor. Fiz.*, **37**: 1819 (1959) (in Russian).
66. R. J. Weiss, *Proc. Phys. Soc.*, **82**: 281 (1963).
67. A. Z. Men'shikov, S. K. Sidorov, and V. E. Arkhipov, *Zh. Eksp. Teor. Fiz.*, **61**: 311 (1971) (in Russian).
68. B. R. Coles, R. H. Taylor, B. V. B. Sarkissian et al., *Physica B*, **86–88**: 275 (1977).
69. J. L. Moran-Lopez and L. M. Falicov, *J. Phys. C: Solid State Phys.*, **13**: 1715 (1980).
70. J. Urias and J. L. Moran-Lopez, *Phys. Rev. B*, **26**: 2669 (1982).
71. J. M. Sanchez and C. H. Lin, *Phys. Rev. B*, **30**: 1448 (1984).
72. P. L. Rossiter and P. J. Lawrence, *Phil. Mag. A*, **49**: 535 (1984).
73. P. J. Lawrence and P. L. Rossiter, *J. Phys. F: Met. Phys.*, **16**: 543 (1986).
74. M. C. Cadeville and J. L. Moran-Lopez, *Physics Reports*, **153**: 331 (1987).
75. J. B. Staunton, D. D. Johnson, and B. L. Gyorffy, *J. Appl. Phys.*, **61**: 3693 (1987).
76. D. D. Johnson, F. J. Pinski, and J. B. Staunton, *J. Appl. Phys.*, **61**: 3715 (1987).
77. M. B. Taylor, B. L. Gyorffy, and C. J. Walden, *J. Phys.: Condens. Matter*, **3**: 1575 (1991).
78. M. B. Taylor and B. L. Gyorffy, *J. Magn. Magn. Mater.*, **104–107**: 877 (1992).
79. M. Dubé, P. R. L. Heron, and D. G. Rancourt, *J. Magn. Magn. Mater.*, **147**: 122 (1995).
80. M.-Z. Dang, M. Dubé, and D. G. Rancourt, *J. Magn. Magn. Mater.*, **147**: 133 (1995).
81. M.-Z. Dang and D. G. Rancourt, *Phys. Rev. B*, **53**: 2291 (1996).
82. A. Z. Men'shikov and E. E. Yurchikov, *Izv. Akad. Nauk SSSR. Ser. Fiz.*, **36**: 1463 (1972) (in Russian).
83. M. Hatherly, K. Hirakawa, R. D. Lowde et al., *Proc. Phys. Soc.*, **84**: 55 (1964).
84. T. Maeda, H. Yamauchi, and H. Watanabe, *J. Phys. Soc. Japan*, **35**: 1635 (1973).
85. V. A. Tatarenko and K. L. Tsinman, *Metallofizika*, **14**: 14 (1992) (in Russian).

86. D. de Fontaine, *Acta Metall.*, **23**: 553 (1975).
87. J. M. Sanchez, D. Gratias, and D. de Fontaine, *Acta Crystallogr. A*, **38**: 214 (1982).
88. V. N. Bugaev and R. V. Chepul'skii, *Acta Crystallogr. A*, **51**: 456 (1995); V. N. Bugaev and R. V. Chepul'skii, *Acta Crystallogr. A*, **51**: 463 (1995).
89. A. A. Abrahamson, *Phys. Rev.*, **178**: 76 (1969).
90. A. V. Ruban, S. Khmelevskyi, P. Mohn, and B. Johansson, *Phys. Rev. B*, **76**: 014420-1 (2007).
91. G. Bonny, R. C. Pasianot, and L. Malerba, *Modelling Simul. Mater. Sci. Eng.*, **17**: 025010-1 (2009).
92. A. G. Khachaturyan, *Fiz. Tverd. Tela*, **4**: 2840 (1962) (in Russian).
93. A. G. Khachaturyan, *Fiz. Tverd. Tela*, **9**: 2861 (1967) (in Russian).
94. H. E. Cook and D. de Fontaine, *Acta Metall.*, **17**: 915 (1969).
95. H. E. Cook and D. de Fontaine, *Acta Metall.*, **19**: 607 (1971).
96. T. J. Matsubara, *J. Phys. Soc. Japan*, **7**: 270 (1952); H. Kanzaki, *J. Phys. Chem. Solids*, **2**: 24 (1957); M. A. Krivoglaz, *Zh. Eksp. Teor. Fiz.*, **34**: 204 (1958) (in Russian).
97. V. N. Bugaev and V. A. Tatarenko, *Interaction and Arrangement of Atoms in Interstitial Solid Solutions Based on Closed-Packed Metals* (Kiev: Naukova Dumka: 1989) (in Russian).
98. V. A. Tatarenko and V. M. Nadutov, *Uspehi Fiziki Metallov*, **5**: 503 (2004) (in Ukrainian).
99. S. V. Beiden and V. G. Vaks, *Physics Letters A*, **163**: 209 (1992).
100. M. S. Blanter, *Phys. Stat. Sol. B*, **181**: 377 (1994).
101. M. S. Blanter, J. *Alloys and Compounds*, **282**: 137 (1999).
102. M. S. Blanter, J. *Alloys and Compounds*, **291**: 167 (1999).
103. C. Wolverton, V. Ozoliņš, and A. Zunger, *Phys. Rev. B*, **57**: 4332 (1998).
104. H. Reichert, V. N. Bugaev, O. Shchyglo et al., *Phys. Rev. Lett.*, **87**: 236105-1 (2001); O. Shchyglo, A. Días-Ortiz, A. Udyansky et al., *J. Phys.: Condens. Matter*, **20**: 045207-1 (2008).
105. W. B. Pearson, *Handbook of Lattice Spacing and Structure of Metals and Alloys* (New York: Pergamon Press: 1958), vol. **1**; W. B. Pearson, *Handbook of Lattice Spacing and Structure of Metals and Alloys* (New York: Pergamon Press: 1968), vol. **2**.
106. J. Zarestky and C. Stassis, *Phys. Rev. B*, **35**: 4500 (1987).
107. R. J. Birgeneau, J. Cordes, G. Dolling, and A. D. B. Woods, *Phys. Rev. A*, **136**: 1359 (1964).
108. S. Lefebvre, F. Bley, M. Bessiere et al., *Acta Crystallogr. A*, **36**: 1 (1980).
109. S. Lefebvre, F. Bley, M. Fayard, and M. Roth, *Acta Metall.*, **29**: 749 (1981).
110. F. Bley, Z. Amilius, and S. Lefebvre, *Acta Metall.*, **36**: 1643 (1988).
111. G. E. Ice, C. J. Sparks, A. Habenschuss, and L.B. Shaffer, *Phys. Rev. Lett.*, **68**: 863 (1992).
112. X. Jiang, G. E. Ice, C. J. Sparks, and P. Zschack, *Mat. Res. Soc. Symp. Proc.*, **375**: 267 (1995).
113. X. Jiang, G. E. Ice, C. J. Sparks et al., *Phys. Rev. B*, **54**: 3211 (1996).
114. G. E. Ice, C. J. Sparks, J. L. Robertson et al., *Mat. Res. Soc. Symp. Proc.*, **437**: 181 (1996).
115. G. E. Ice, G. S. Painter, L. Shaffer et al., *NanoStructured Materials*, **7**: 147 (1996).
116. G. E. Ice, C. J. Sparks, X. Jiang, and J. L. Robertson, *J. Phase Equil.*, **19**: 529 (1998).

117. G. E. Ice and C. J. Sparks, *Annu. Rev. Mater. Sci.*, **29**: 25 (1999).
118. J. L. Robertson, G. E. Ice, C. J. Sparks et al., *Phys. Rev. Lett.*, **82**: 2911 (1999).
119. P. Cenedese, F. Bley, and S. Lefebvre, *Mat. Res. Soc. Symp. Proc.*, **21**: 351 (1984).
120. F. Livet, *Acta Metall.*, **35**: 2915 (1987).
121. A. G. Khachaturyan, *Fiz. Tverd. Tela*, **9**: 2594 (1967) (in Russian); A. G. Khachaturyan, *Fiz. Tverd. Tela*, **11**: 3534 (1969) (in Russian).
122. H. E. Cook, *J. Phys. Chem. Solids*, **30**: 2427 (1969); H. E. Cook, D. de Fontaine, and J.E. Hillard, *Acta Metall.*, **17**: 765 (1969); H. E. Cook, *Acta Metall.*, **18**: 297 (1970).
123. M. A. Krivoglaz and S. P. Repetskii, *Fiz. Tverd. Tela*, **8**: 2908 (1966) (in Russian).
124. M. M. Naumova, S. V. Semenovskaya, and Y. S. Umanskii, *Fiz. Tverd. Tela*, **12**: 975 (1970) (in Russian); M. M. Naumova and S. V. Semenovskaya, *Fiz. Tverd. Tela*, **12**: 3632 (1970) (in Russian).
125. V. A. Tatarenko and T. M. Radchenko, *Metallofiz. Noveishie Tekhnol.*, **24**: 1335 (2002) (in Ukrainian); V. A. Tatarenko and T. M. Radchenko, *Uspehi Fiziki Metallov*, **3**: 111 (2002) (in Ukrainian).
126. S. M. Bokoch, N. P. Kulish, V. A. Tatarenko, and T. M. Radchenko, *Metallofiz. Noveishie Tekhnol.*, **26**: 387 (2004) (in Russian); S. M. Bokoch, N. P. Kulish, V. A. Tatarenko, and T. M. Radchenko, *Metallofiz. Noveishie Tekhnol.*, **26**: 541 (2004) (in Russian); S. M. Bokoch, N. P. Kulish, and T. D. Shatnii, *Metallofiz. Noveishie Tekhnol.*, **26**: 627 (2004) (in Russian); T. M. Radchenko, V. A. Tatarenko, and S. M. Bokoch, *Metallofiz. Noveishie Tekhnol.*, **28**: 1699 (2006); S. M. Bokoch, N. P. Kulish, and V. A. Tatarenko, *Fundamental. Problemy Sovremen. Materialoved.*, **4**: 78 (2007) (in Russian); S. M. Bokoch, M. P. Kulish, V. V. Ryashko, and V. A. Tatarenko, *Functional Materials*, **14**: 92 (2007); S. M. Bokoch, D. S. Leonov, M. P. Kulish, V.A. Tatarenko, and Yu.A. Kunitsky, *Phys. Stat. Sol. A*, **206**: 1766 (2009).
127. V. I. Goman'kov, I. M. Puzei, V. N. Sigaev et al., *Pisma Zh. Eksp. Teor. Fiz.*, **13**: 600 (1971) (in Russian); A. Z. Men'shikov, V. Ye. Arkhipov, A. I. Zakharov, and S. K. Sidorov, *Fiz. Met. Metalloved.*, **34**: 309 (1972) (in Russian).
128. V. I. Goman'kov, N. I. Nogin, and E. V. Kozis, *Metally*, **12**: 174 (1982) (in Russian); V. I. Goman'kov, N. I. Nogin, and E. V. Kozis, *Fiz. Met. Metalloved.*, **55**: 125 (1983) (in Russian).
129. B. Schönfeld, *Prog. Mater. Sci.*, **44**: 435 (1999).
130. H. Chen and J. B. Cohen, *Acta Metall.*, **27**: 603 (1979).
131. S. M. Bokoch, V. A. Tatarenko, and I. V. Vernyhora (to be published).
132. F. Ono, H. Maeta, and L. Bang, *J. Magn. Magn. Mater.*, **140–144**: 247 (1995).
133. Y. Tsunoda, L. Hao, S. Shimomura et al., *Phys. Rev. B*, **78**: 094105-1 (2008).
134. I. B. Ramsteiner, O. Shchyglo, M. Mezger et al., *Acta Mater.*, **56**: 1298 (2008).
135. C. J. Sparks, G. E. Ice, X. Jiang, and P. Zschack, *Applications of Synchrotron Radiation Techniques to Materials Science II*, vol. **375** (Eds. L. J. Terminello, N. D. Shinn, G. E. Ice, K. L. D'Amico, and D. L. Perry) (Pittsburgh: PA, MRS: 1995), p. 213.
136. G. E. Ice, C. J. Sparks, and L. B. Shaffer, *Resonant Anomalous X-Ray Scattering* (Eds. G. Materlik, C.J. Sparks, and K. Fischer) (Amsterdam: North-Holland: 1994), p. 265.
137. G. E. Ice, C. J. Sparks, L. B. Shaffer, and P. Zschack, *Alloy Modeling and Design* (Eds. G. M. Stocks and P. E. A. Turchi) (Warrendale: PA, TMS Mineral Metals and Materials: 1994), p. 215.